



HAL
open science

Stranded in the high tide line: spatial and temporal variability of beached microplastics in a semi-enclosed embayment (Arcachon, France)

Charlotte Lefebvre, Isabel Jalón-Rojas, Juliette Laserre, Sandrine Villette, Sophie Lecomte, Jérôme Cachot, Bénédicte Morin

► To cite this version:

Charlotte Lefebvre, Isabel Jalón-Rojas, Juliette Laserre, Sandrine Villette, Sophie Lecomte, et al.. Stranded in the high tide line: spatial and temporal variability of beached microplastics in a semi-enclosed embayment (Arcachon, France). *Science of the Total Environment*, 2021. hal-03783877

HAL Id: hal-03783877

<https://hal.science/hal-03783877>

Submitted on 22 Sep 2022

HAL is a multi-disciplinary open access archive for the deposit and dissemination of scientific research documents, whether they are published or not. The documents may come from teaching and research institutions in France or abroad, or from public or private research centers.

L'archive ouverte pluridisciplinaire **HAL**, est destinée au dépôt et à la diffusion de documents scientifiques de niveau recherche, publiés ou non, émanant des établissements d'enseignement et de recherche français ou étrangers, des laboratoires publics ou privés.

1 **Stranded in the high tide line: spatial and temporal variability of beached microplastics**
2 **in a semi-enclosed embayment (Arcachon, France)**

3

4

5 Charlotte Lefebvre^{1,2}, Isabel Jalón Rojas¹, Juliette Lasserre¹, Sandrine Villette ², Sophie
6 Lecomte², Jérôme Cachot¹, Bénédicte Morin^{1*}

7

8 ¹ EPOC, University of Bordeaux, CNRS, OASU, EPHE, UMR 5805, 33600 Pessac, France

9 ² CBMN, University of Bordeaux, CNRS, Bordeaux INP, UMR 5248, 33600, Pessac, France

10

11 *Corresponding author

12 Email address: benedicte.morin@u-bordeaux.fr

13 UMR CNRS 5805 EPOC-OASU - Bâtiment B2, allée Geoffroy Saint-Hilaire, CS50023 -
14 33615 Pessac Cedex, France

15

16

17 Preference for color:

18 Online version only

19

20

21 Abstract

22 Coastal environments are a predominant ultimate destination of marine debris, becoming a
23 key focus of studies assessing microplastic (MP) contamination. Here, we described the visible
24 fraction of MP (from 0.5 to 5 mm) that washed up during the high tide at different sites of a
25 semi-enclosed mesotidal bay and investigated the main abiotic factors driving MP beaching.

26 Three contrasted beaches of the Arcachon Bay (SW France) were monitored on a monthly basis
27 during 2019. Samplings were made along a 100 m longitudinal transect at the high-water
28 strandline (4 quadrats of 0.25m²) and at an intermediate tidal range. Each sampled particle was
29 characterized by morphometric data (e.g. size, shape, color, roughness) and polymer
30 identification was performed by ATR-FTIR technique. Results show that MP concentration was
31 higher on the beach located at the mouth of the bay (36.0 ± 39.2 MP.m⁻²) than at the back and
32 the outside of the bay (respectively 2.7 ± 4.4 and 1.7 ± 2.4 MP.m⁻²). This may be related to the
33 strong currents at the entry of the embayment and the beach orientation, exposed to predominant
34 winds. Beached MP were mainly pre-production pellets and fragments as they represented
35 respectively 49 % and 39 % of all analyzed shapes. Polymers with low density were particularly
36 abundant. Polyethylene represented 69 % of all the particles while polypropylene accounted for
37 17 % and polystyrene for 10 %. We also observed that MP were mostly washed up when wind,
38 waves and river flow were more intense. Analysis suggest that wind direction and speed are
39 key factors influencing beaching as strong onshore wind enhance this process.

40

41 Key-words: microplastic, beaching, quantification, identification, environmental factors,
42 Atlantic coast

43

44

45 **Introduction**

46

47 Since its discovering in 1950s, plastic is omnipresent in our everyday life. Its use is
48 unavoidable in all industries such as packaging, building, electronic, textile or agriculture.
49 “Plastic materials” expression commonly refers to various synthetic polymer types in which
50 many additives such as flame retardants or stabilizers can be included (Thompson et al., 2009).

51 In 2015, 380 million tons of plastic were produced worldwide (Geyer et al., 2017) and since the
52 beginning of plastic production, around 4900 million tons already entered the natural
53 environment, which is equivalent to 60% of all plastics ever produced (Geyer et al., 2017).
54 Moreover, plastic litter is recognized as being ubiquitous in the marine environment (Jeftic et
55 al., 2009). This pollution is now raising serious concerns about environmental, economic,
56 aesthetical and societal issues (Bergmann et al., 2015; Goverse et al., 2014; Moore, 2008).

57

58 Estimations based on modeling indicate that 5 trillion of plastic particles are floating at
59 the surface of the ocean, 92.4 % of them being particles with dimensions between 0.33 mm and
60 4.75 mm (Eriksen et al., 2014). Actually, authors have assigned different size categories of
61 plastic litter. Microplastic (MP) category commonly refers to pieces which have a size inferior
62 to 5 mm (Gago et al., 2016; Marine Strategy Framework Directive, 2013). Lower limit size,
63 which makes the distinction with nanoplastics particles, can vary between 1 μm (da Costa et
64 al., 2016) and 100 μm (Bergmann et al., 2015) among studies and working groups. Recently,
65 Frias and Nash (2019) proposed a consensual definition: “*Microplastics are any synthetic solid*
66 *particle or polymeric matrix, with regular or irregular shape and with size ranging from 1 μm*
67 *to 5 mm, of either primary or secondary manufacturing origin, which are insoluble in water*”.

68 A common size range definition is crucial for consistency and comparison between studies.
69 Besides, MP can be described by a secondary origin when they come from fragmentation and
70 degradation of larger plastic pieces (Cole et al., 2011; GESAMP, 2015). On the contrary,
71 primary MP have two major origins, they are either plastic particles manufactured at small size
72 (GESAMP, 2015), or discarded in the environment at a small size (inferior to 5 mm; Boucher
73 and Friot, 2017). MP are also commonly described by their shape (e.g. pellets, fragments, foams,
74 fibers) and color (e.g. white, black, blue, red) (e.g. Hidalgo-Ruz et al., 2012; Lusher et al., 2020).

75

76 Once in the marine environment, MP are known to adsorb hydrophobic chemicals
77 (Engler, 2012). Consequently, organic pollutants such as PCBs and PAHs have been found on
78 MP (pellets and fragments) collected on sandy beaches (e.g. Gorman et al., 2019; Ogata et al.,
79 2009) but also other contaminants like metals (e.g. Massos and Turner, 2017). Moreover, MP
80 can be ingested by a large diversity of marine organisms, such as invertebrates (e.g. Courteney-
81 Jones et al., 2019), seabirds (e.g. Amélineau et al., 2016; Baak et al., 2020) and turtles (e.g.
82 Duncan et al., 2019; Matiddi et al., 2019). Chemicals that are associate to MP are bioavailable
83 and can impair early stage development of different species (e.g. Cormier et al., 2021; Pannetier
84 et al., 2020; Scopetani et al., 2018) but can also be transferred to upper trophic level (Cousin et
85 al., 2020).

86

87 MP fragmentation process seems to occur preferentially in specific systems such as
88 beaches given that they are exposed to UV radiation, wave and wind actions and in some places
89 to tidal cycles (e.g. Andrady, 2011; Cooper and Corcoran, 2010; Corcoran et al., 2009).
90 Moreover, beaches are likely to be a hot spot for plastic among all litter types as it could make
91 up 92% of total recovered litter (Vlachogianni et al., 2018). For example, observations of
92 exceptional high concentrations, up to 258 408 items per m², has been reported at one beach of
93 Lantau Island (Hong-Kong, Fok and Cheung, 2015). Turra et al. (2015) also suggested that
94 deposition on sandy beaches may be the predominant fate of MP, including pre-production
95 pellets. Despite the multiplication of sampling surveys on beaches over the last years (e.g.
96 Carvalho et al., 2021; Pérez-Alvelo et al., 2021; Tata et al., 2020), the temporal and spatial
97 variabilities in the distribution and transport patterns of MP are not yet clearly understood for
98 this compartment. This may be related to the lack of recurrent (e.g. monthly) multi-site
99 monitoring and the multiple environmental and anthropic factors influencing the MP beaching
100 process at different time scales. Indeed, anthropic factors that influence variabilities of MP

101 contamination of beaches include, for instance, the distance to an industrial or urban center or
102 proximity to port facilities (e.g. Antunes et al., 2018; Hidalgo-Ruz and Thiel, 2013). The
103 closeness and density of anthropic activities tend as well to increase concentration of MP
104 according to previous studies (e.g. Browne et al., 2011; Hidalgo-Ruz and Thiel, 2013).
105 Variations in beached MP concentrations at global, regional and local scales may also be
106 influenced by environmental parameters such as the proximity to a river mouth (e.g. Constant
107 et al., 2019; Karthik et al., 2018; Williams et al., 2016), the river influx of microplastics (Karthik
108 et al., 2018) and hydrodynamics features (e.g. Balthazar-Silva et al., 2020; Williams et al.,
109 2017). In coastal and nearshore waters, tidal currents, wind-driven currents, wave processes
110 (shoaling, breaking) and their related currents may affect the behavior, transport and beaching
111 of MP (Forsberg et al., 2020; Jalón-Rojas et al., 2019a; Zhang, 2017). Beaching and MP
112 concentration on shoreline may also depend on beach-specific factors such as the specific
113 exposure and morphology (e.g. beach profile, slope, topography, beach rock) (e.g. Lo et al.,
114 2020; Pinheiro et al., 2019; Ryan et al., 2018).

115 An accurate estimation of fluxes and modelling of transport pathways requires
116 qualitative and quantitative assessment of standing stock of MP in all aquatic compartments
117 (regardless of the size range of particles). For instance, deposition and recapturing processes
118 are known, but not systematically considered in modeling studies due to the lack of data to
119 implement this process. Actually, studies often sampled MP within the sediment. Yet, the
120 fraction of “large” MP (1-5 mm) that freshly washed up onto the beach is rarely described
121 specifically (e.g. Antunes et al., 2018). However, this fraction may help to evaluate MP standing
122 stock and inputs in this compartment, as well as to assess the complex dynamic and high
123 variabilities even at a local scale. It also may reflect, at least partially, what is floating at the sea
124 surface near the coastline before being transport by tides to the beach. Additionally, the Marine
125 Strategy Framework Directive (MSFD) Technical Subgroup on Marine Litter (TSG-ML)

126 recommends to study beach litter distribution (including MP) and its variations in order to
127 support management policies and evaluate efficiency of mitigation strategies (Marine Strategy
128 Framework Directive, 2013). Moreover, beached MP surveys are not expensive, do not
129 necessitate complicated preparations and analysis time is shorter when considering only the
130 visible fraction. Still, it provides reliable data for the description in the environment but also
131 for models inputs.

132

133 In this overall context, this paper reported the description of MP beaching at three
134 different locations of the Arcachon Bay (South-West, France) by conducting monthly sampling
135 over one year. This triangular-shaped lagoon, connected to the Atlantic Ocean, is mainly
136 influenced by a semi diurnal tidal cycle (Plus et al., 2009). It is also a place supporting several
137 anthropic pressures like growing urbanization, fishing, shell farming and a strong seasonal
138 tourist activity. The study focuses on MP that freshly beached with the high tide line at an
139 intermediate tidal range for the Atlantic coast. Besides, this study takes into account
140 environmental factors such as wind, wave and river flow during the whole sampling period to
141 better understand MP deposition in this area. Therefore, this research aims to (1) make a
142 quantitative and qualitative analysis of MP deposition on three different beaches in the
143 Arcachon Bay, (2) evaluate the spatial and temporal variability in MP distribution over one year
144 and (3) evaluate the influence of environmental factors on MP beaching variability.

145

146 **Methods**

147

148 2.1 Studied area

149 The Arcachon bay is a lagoon located on the South West coast of France and connected
150 to the Atlantic Ocean (44°40'N, 1°10'W; Fig. 1A). This triangular shaped lagoon extends over

151 a surface of 160 Km² at high tide (Cayocca, 2001). A complex network of channels and
152 intertidal flats characterizes the inner bay. At the mouth, two main channels called North and
153 South channels connect the bay to the ocean and make the water circulation possible (Fig. 1A).
154 Tides are semidiurnal and dominate the hydrodynamic in both the inner bay and inlet (Plus et
155 al., 2009; Salles et al., 2015). Tidal range oscillates between 0.80 m and 4.60 m (Cayocca, 2001)
156 and the mean tidal prism is 384 million m³, meaning here that two third of the water volume is
157 renewed during each tidal cycle (Plus et al., 2009). Winds are also a major factor influencing
158 the hydrodynamic of the bay, the strongest coming frequently from the west and north-west
159 (onshore winds hereafter) (IFREMER, 2007). Strong currents (up to 2 m.s⁻¹) occur at the inlet
160 and main channels while they are weaker (below 0.5 m.s⁻¹) outside the bay and in intertidal
161 areas (Plus et al., 2009). General water circulation displays a major marine water inflow by the
162 South channel and a major outflow by the North Channel (Salles et al., 2015). The outer bay is
163 influence by waves with wave height ranging from 0.1 to about 10 m (Castelle et al., 2007).
164 The Leyre river is the major contributor to continental water input in the bay (Plus et al., 2009)
165 with a mean annual flow of 17.30 m³.s⁻¹ (calculated over the past 55 years,
166 <http://www.hydro.eaufrance.fr/>, last visit on May 3rd 2021).

167 The Arcachon bay supports several anthropic activities that are economically important
168 for the region, such as oyster farming and spat collection and sale. There is also professional
169 and recreational fishing all year long. The Arcachon bay is also a major touristic destination
170 welcoming more than 750,000 people per year (from April to September). The recreational use
171 of the marine area, such as sailing, is increasing at this season. Additionally, this region is
172 becoming more and more attractive; as a result, local population and urbanization are increasing.
173 In 2017, around 150,000 residents lived around the Arcachon Bay (National Institute of
174 Statistics and Economic Studies, population census of 2017) while in 2006 they were 130,000
175 residents. Besides, sewage from five wastewater treatment plants (among which one is

176 industrial and the others are urban ones) discharge in the ocean by a wastewater drainage pipe
177 named Wharf (Fig. 1A). The mean daily flow of the Wharf is 60,000 m³ among which half of
178 the volume came from the industrial wastewater treatment plant. Industrial wastewater is
179 coming from a manufacturer of paper-based packaging that use pine cellulose from the local
180 forest.

181

182 2.2 Field measurements

183

184 2.2.1 Sampling of MP

185 The three studied beaches are sandy. According to precedent studies (Lorin & Viguiet
186 1987, Sénéchal et al., 2009), grain size on beaches around Arcachon Bay is around 350 µm so
187 they are categorized as medium-grained. The first beach is located outside of the bay, the second
188 at its mouth and the third one at the back of the bay (Fig. 1A). The outside station (OS) is an
189 oceanic beach directly exposed to high-energy waves and onshore winds. The mouth station
190 (MS) is also exposed to onshore winds and is located on the South Channel where strong
191 currents occur. Finally, the back station (BS) is located in a region mainly dominated by tides
192 and close to the Leyre river outlet. Samplings were made each month from January 2019 to
193 December 2019 at an intermediate tidal range (around 3 - 3.5 m) to minimize the variability
194 due to the spring-neap tidal cycle. From May to September, the municipality cleans MS beach
195 every day. To minimize the effect of cleaning on data collection, samplings were made just after
196 the end of the high tide and before the cleaning. The sampling protocol was based on MSFD
197 guidance (e.g. same sampling day between sites, reference points, no jetties or breakwater, no
198 impact on local species) (Marine Strategy Framework Directive, 2013) and recommendations
199 made by the Cedre (Center of documentation, research and experimentation on accidental water
200 pollution) for the sampling of MP on sandy beach of the Atlantic Ocean (e.g. same tidal range,

201 transect length). Sampling protocol was adapted in order to make a focus solely on MP that
202 were freshly deposited onto the beach by the last high tide. Dates of sampling were chosen
203 according to tidal range and the hour of the first high tide, that had to be early in the morning.
204 As such, the three studied sites were sampled on the same day after the first high tide of the day
205 and before the second high tide of the day. The high tide mark was carefully identified by
206 checking humidity within the tide line (e.g.: shell with water, wet sea grass blades), the sand
207 humidity and uniformity (over the last high tide line sand was dry and many footprints were
208 visible while under the last tide line there were no or few footprints and sand grains were
209 flattened by the water tidal movement). Along a 100 m longitudinal transect, a quadrat of 0.50
210 m length sides (0.25 m²) was laid on the tide line at 25 m, 50 m, 75 m and 100 m (Fig. 1B).
211 GPS coordinates were taken at the beginning and the end of the transect (0 and 100 m). In total,
212 1 m² of the high tide line was meticulously inspected at each site for MP collection. Inspection
213 was conducted by checking the quadrat surface, firstly without disturbance and secondly by
214 checking each organic or mineral item constituting the tide line and removing them to check
215 also if plastic-like items were not hidden by other materials. All suspected plastic microparticles
216 (e.g. colored items, hardly breakable, no ornamentation, no squeaking under stainless steel
217 pliers) that were visible from the naked eyes (from 0.5 to 5 mm) were recovered and then kept
218 in ziplock plastic bags corresponding to the sampled quadrat.

219

220 1.2.2 Environmental data collection

221 *In situ* hydrodynamics and meteorological data from local monitoring networks or
222 numerical models were collected and analyzed to gain further understanding of the spatial and
223 temporal variability of MP beaching and of the role of environmental drivers on it. In particular,
224 5 datasets covering the studied period, from December 2018 to December 2019, were
225 considered:

- 226 a. Hourly water level measurements at Eyrac station (Fig. 1A), provided by the French
227 Naval Hydrographic and Oceanographic Service (SHOM). Tidal range (TR) was
228 calculated from this dataset as the difference between high and low waters.
- 229 b. Hourly wind speed (Uwind) and direction observations at Cap-Ferret station (Fig.
230 1A) provided by the French national meteorological service (METEO France).
- 231 c. Hourly significant wave height (HS) and dominant wave direction (DP) at Cap-
232 Ferret CANDHIS station (44.6525, -1.446667), provided by the HOMERE wave
233 hindcast database (Boudière et al., 2013) and recalibrated using past observations
234 from the French CANDHIS dataset at this same station. Readers can refer to
235 Castelle et al. (2020) for a detailed explanation of the recalibration method.
- 236 d. Hourly surface current velocities in the Bay of Biscay based on numerical
237 simulations with MARS2D, provided by the Modeling and Analysis for Coastal
238 Research MARC (spatial resolution : 250 m, Rank 2; Pineau-Guillou, 2013).
- 239 e. Daily river discharge (Q) recorded at Salles (44.548112, -0.871571), supplied by the
240 DREAL Aquitaine and available on the French National database Banque Hydro.

241

242 2.3 Sample analysis

243

244 2.3.1 Visual and chemical characterizations of MP

245 During analysis, nitrile gloves and 100% cotton lab coat were worn, the lab bench and
246 tools were cleaned with 70 % filtered Ethanol, aluminum containers and stainless steel pliers
247 were used to sort and handle particles. As recommended by the Marine Strategy Framework
248 Directive (2013), size (length and width), shape (i.e. pellet, fragment, film, fiber/filament or
249 foam; photos in Fig. S1), a sub category of shape (e.g. for pellet particles: cylindrical, spheroid,
250 pressed and flat; for fragment particles: rounded, sub-angular and angular), opacity (i.e.

251 transparent or opaque), color (e.g. white, blue, black, yellow, green,...) and surface particle's
252 roughness (i.e. smooth or rough) were recorded for each sampled particle. Hereafter, data for
253 shapes, colors and sizes refer to this visual characterization of particles. Particles were measured
254 under the binocular (Micros AUSTRIA MS 1107, magnification range: x10 - x30) with a graph
255 paper. Items were weighted for each shape category of each quadrat (Mettler Toledo AE240S;
256 scale division: 0.1 mg) and then summed up to obtain the overall weigh of particles from each
257 quadrat.

258 The chemical characterization of MP was performed using a Fourier-Transform Infrared
259 (FTIR) spectrometer (Nicolet, Nexus 870) equipped with an MCT detector with an Attenuated
260 Total Reflectance (ATR) diamond crystal accessory (Pike technology, MIRacle). All spectra
261 were recorded at a resolution of 4 cm⁻¹ over the range 4000-600 cm⁻¹ and analyzed with OMNIC
262 software (ThermoFisher, V9.2.98). Among the 500 items that were collected throughout the
263 year and visually characterized, 86% (430 items) were analyzed by ATR-FTIR (see Table 1 for
264 details by site). Most of the sampled items were large and thick enough to provide a great quality
265 of spectra with good signal to noise ratio (except for two particles that were excluded of the
266 study). Automatic baseline correction was performed on each spectrum. The spectra were then
267 matched to different libraries (described in Table S1) provided by Thermo Fisher to assign a
268 chemical composition. A manual validation of the identified polymer was made for each item
269 (e.g. presence and matching of the characteristic absorption bands, recurrence of the listed
270 polymers). Each synthetic polymer was listed under its own name (e.g. polyethylene), mineral
271 and cellulosic compounds were gathered to form the category "non-plastic" (NP) and items that
272 were not identified were listed as unknown category (UNK). Spectra of each polymer type of
273 MP are available in Figure S2, together with the corresponding spectra of the polymer in the
274 reference library.

275

276

277 2.3.2 Correction of the MP concentration

278 As only a fraction of items was analyzed by ATR-FTIR, we corrected MP
279 concentrations for each month to take into account MP that have been visually described but
280 not chemically identified. We used the following calculation (eq.1):

$$281 \quad [MP]_{corrected} = Tot_{MP} \times \frac{Tot_{item}}{Tot_{FTIR}} \quad (1)$$

282 where $[MP]_{corrected}$ corresponds to the corrected concentration of MP (in $MP \cdot m^{-2}$), Tot_{MP}
283 represents the total amount of chemically identified MP, Tot_{item} corresponds to the total amount
284 of particles that were sampled, and Tot_{FTIR} represents the total amount of items that were
285 analyzed by ATR-FTIR. In the following text, all MP concentration data refer to the corrected
286 concentrations.

287

288 2.4 Data analysis

289 The map of the sampling locations was made with the ArcGis software (V10.7.1).
290 Statistical analyses were performed with the R software (RStudio Team, 2016; V1.1.463). The
291 packages “ggplot2” (Wickham, 2016) and “ggpubr” (Kassambara, 2020) were employed to
292 generate figures. Distribution data did not fulfill normality and homoscedasticity assumptions
293 that are required for parametric tests. As such, non-parametric tests were running to analyze the
294 spatial variability. The Kruskal-Wallis (H-test) test was performed to test the null hypothesis
295 (H_0) of similar dimension's (i.e. width and length) and similar MP concentration between sites.
296 When differences between factors were noticed, the Wilcoxon test (W-test) was performed
297 (significance level, 0.05). The Fisher-exact test was done to compare colors, shapes and
298 polymers proportions between two factors as these variables often display a headcount of less
299 than five (significance level, 0.05). The null hypothesis (H_0) tested was that morphometric data
300 of polymer types proportions would be equally distributed between sites.

301 The temporal evolution of the MP abundance and the different environmental
302 parameters were compared through time-series analysis, Pearson correlation coefficient
303 calculation and principal component analysis (PCA). For this purpose, we considered the values
304 of the environmental parameter at the moment of each sampling but also weighted averaged
305 values of current velocities, wind speed, significant wave heights and river flow over the
306 precedent 10 days following eq. 2, which gives more weight to data closer to the sampling date:

$$307 \quad P_{mean} = \frac{\sum_{j=0}^{2\Phi\Delta t} P_j 10^{-j\Delta t/\Phi}}{\sum_{j=0}^{2\Phi\Delta t} j=0} \quad (2)$$

308 where P_{mean} is the weighted averaged value of the environmental parameter P ; j is the
309 number of data points prior to the calculation point ($j=0$); Δt the sampling interval (days); and
310 Φ is the memory decay of the system meaning that Φ is the number of days in the past when
311 the exponentially decaying weighting factor decreases to 10%, with 2Φ taken as a limit for P_{mean}
312 computation (Davidson et al., 2013). These weighted averages are commonly used in coastal
313 physical oceanography for averaging waves (e.g. Castelle et al., 2014; Davidson et al., 2013;
314 Splinter et al., 2013) in order to consider the memory effect of the systems (e.g. significant
315 morphological changes that may occur or big amounts of plastic that may be found on the beach
316 several days after a big storm).

317

318 **Results**

319

320 3.1 Characterization and spatial distribution of beached microplastic

321 Particles' mean length for Outside Station (OS), Mouth Station (MS) and Back station (BS)
322 were respectively 3.5 ± 0.8 mm, 3.4 ± 0.7 mm, 3.5 ± 0.4 mm and mean width were 3.0 ± 1.2
323 mm, 2.8 ± 1.1 mm, 2.6 ± 1.1 mm. There were no differences of particles' dimensions between
324 sites (length, H-test, $N = 500$, p-value = 0.7; width, H-test, $N = 500$, p-value = 0.4). The main
325 recovered length range at all sites was between 3 mm and 4 mm (> 42%) while main width

326 range was 3 – 4 mm at OS (36.4%), 2 – 3 mm at MS (34.3%) and 1 – 2 mm at BS (37.9%; Fig.
327 S3). Mean total weight of particles was $21.0 \pm 41.6 \text{ mg.m}^{-2}$ at the OS, $584.2 \pm 743.4 \text{ mg.m}^{-2}$ at
328 MS and $32.4 \pm 68.5 \text{ mg.m}^{-2}$ at BS (Table S2).

329

330 Pellets particles represented 45.5% of all collected items at OS, 50.3% at MS and 34.3% at
331 BS (Fig. 2A). The main subcategory of shape among pellets items was the flat/disk one (at least
332 40.8%) while cylindrical pellets constituted at least 25.1% (Table S3). The second most
333 described general shape was fragment (27.3% at OS, 40.9 % at MS and 34.3% at BS). A greater
334 proportion of foam was found at OS and BS (respectively 22.7% and 22.9%) while it was only
335 8.1% at MS. Fibers constituted 4.5%, 0.5% and 2.8% of particles found respectively at OS, MS
336 and BS. Films were also found in limited proportions as they made up 0%, 0.2% and 5.7% of
337 all particles, respectively at OS, MS and BS (Fig. 2A). There were no differences in the global
338 shape composition of particles between sites (Fisher's exact test, $N = 12$, $p\text{-values} > 0.3$).

339

340 Regarding opacity characteristic, transparent particles were slightly more numerous than
341 opaque ones at MS (64.8%), on the contrary to proportions found at OS and BS (respectively
342 54.5% and 57.1% of opaque particles). White-colored particles were predominant whatever the
343 site (from 46% to 73%; Table 2) while blue items were the second color described (from 9.9%
344 to 28.6%; Table 2). Particles' surface was mainly smooth (from 53.5% to 68.2%). Regarding
345 the global composition of colors, there were no differences between the three sites (Fisher's
346 exact test, $N = 12$, $p\text{-values} > 0.7$) as for transparency and roughness characteristics (Fisher's
347 exact test, $N = 12$, $p\text{-values} > 0.9$).

348

349 Mean concentration of MP was $1.8 \pm 2.4 \text{ MP.m}^{-2}$ at OS, $36.0 \pm 39.2 \text{ MP.m}^{-2}$ at MS and 2.7
350 $\pm 4.4 \text{ MP.m}^{-2}$ at BS (Table 1). MP concentrations were significantly different between sites (H-

351 test, N = 36, p-value = 0.001). MS had a higher MP concentration than at the two others stations
352 (W-test, N = 12, p-values < 0.006; Fig. 3) while OS and BS had similar MP concentrations (W-
353 test, N = 12, p-value = 0.93; Fig. 3). These differences can be related to the particular location
354 of each beach and their exposition to different environmental and hydrodynamic forcing, which
355 is analyzed in Section 3.2 and discussed in detail in Section 4.2.

356

357 Among all items analyzed by ATR-FTIR spectroscopy (N = 430), 96.9% of them were
358 plastic polymers (Table 1), meaning that the visual sorting made on the field was reliable. A
359 vast majority of items were made of polyethylene (PE), as it accounted for 59.1% of all items
360 at OS, 71.2% at MS and 58.8 % at BS (Fig. 2B). Depending on the location, polypropylene (PP)
361 or polystyrene (PS) were the second type of polymer identified. Indeed, PS represented 22.7%
362 and 26.5% of the particles, respectively at OS and BS while it represented only 7.5% at MS
363 (Table S4). Regarding PP, it constituted 13.6%, 17.7%, and 8.8% of analyzed particles,
364 respectively at OS, MS and BS. Even though they were scarce, unusual polymers such as ethyl
365 vinyl acetate (EVA) and poly(isobutyl methacrylate) (PiBMA) were identified at MS
366 (respectively 1.1% and 0.3%). Non-plastic (mineral and cellulosic compounds) made up 4.5%,
367 0.3% and 2.9% of all particles while unknown polymers represented 0%, 1.9% and 2.9%,
368 respectively at OS, MS and BS. Polymer composition were not different between sites (Fisher's
369 exact test, N = 12, p-values > 0.7).

370

371 3.2 Temporal variability of beached MP and influence of environmental factors

372 The monthly variability of MP concentration was relatively important at each site as
373 standard deviations were systematically higher than mean concentrations. All sites displayed an
374 absence of MP at least on one occasion (Table 1, Table S5). In September, all stations displayed
375 a null concentration (Table S5). Maximal concentrations were 8.0 ± 5.6 MP per m^2 at OS (in

376 April), 112.9 ± 63.6 MP per m^2 at MS (in February) and 15.0 ± 6.8 MP per m^2 at BS (in February;
377 Fig. 4A, Table S5). MS showed a more marked seasonality, with a wider concentration range.
378 Overall, MP concentrations tended to be lower from May to September 2019 while it was higher
379 from February to April 2019 and then from October to December 2019 in particular at MS.
380 Unlike the other winter months, MP concentrations were very low in January, except at OS.

381

382 To gain further insight into the temporal and spatial variabilities and trends, we evaluated
383 the temporal evolution of the main environmental factors that may play a role on beaching and
384 dispersion of MP in nearshore water and discussed their potential impact. Figure 4 shows the
385 temporal variability of MP concentrations (Fig. 4A) along with the times series of several
386 environmental factors during the sampling period: tidal range (TR; Fig. 4B), significant wave
387 height (HS; Fig. 4C), wind speed and direction (U_{wind} ; Fig. 4D) and the mean daily flow of the
388 Leyre River (Q; Fig. 4E). The dashed lines highlight sampling days.

389

390 First, we checked that tidal ranges (TR, ranging from 1.3 to 5.0 m) were similar for all the
391 sampling dates (around 3.5 m, Fig. 4B), as planned by the sampling protocol. This confirms the
392 lack of influence of the spring-neap tidal cycle on samplings. Significant wave height (HS)
393 ranged from 0.1 to 4.7 m, with higher values during winter and autumn times (i.e. from January
394 to April and from October to December) and lower values at mid-spring and summer times (i.e.
395 from May to September; Fig. 4C). Westerly winds (onshore winds) were dominant throughout
396 the year and, as for HS, they were more intense in winter and autumn times. Wind speed (U_{wind})
397 ranged between $1.3 \text{ m}\cdot\text{s}^{-1}$ and $17.3 \text{ m}\cdot\text{s}^{-1}$, excluding data recorded after the last sampling day
398 (Fig. 4D). Daily river flow (Q) presented also a similar seasonal variability with lower values
399 in summer (up to $4.3 \text{ m}^3\cdot\text{s}^{-1}$ in September) and higher values around February (up to $36.5 \text{ m}^3\cdot\text{s}^{-1}$)
400 ¹), and then from early November to late December (up to $60.1 \text{ m}^3\cdot\text{s}^{-1}$; Fig. 4E).

401 In general, highest concentrations of beached MP took place during energetic hydrodynamic
402 conditions (i.e. high wind speed, wave height and river discharges), and this was particularly
403 notable in February. MS displayed also high concentrations in November-December which
404 were at least thirty times higher than at OS and BS. Interestingly, the low concentrations
405 observed in January took place during offshore winds, while the maximum concentrations
406 observed in February occurred during onshore winds. This suggests that wind direction plays a
407 key role for MP beaching which will be analyzed in depth in the Discussion (Section 4.2).
408 Pearson correlations between MP concentrations and environmental forcing (for the sampling
409 day and weighted over 10 days, eq. 2) confirmed these trends, particularly at MS (Table S6).
410 Concentrations at MS were positively correlated with Q (sampling day : $r = 0.85$, weighed on
411 10 days : $r = 0.63$, Table S6), HS (sampling day : $r = 0.79$, weighed on 10 days : $r = 0.83$) and
412 U_{wind} in the West-East axis (sampling day : $r = 0.62$, weighed on 10 days : $r = 0.61$). The best
413 Pearson correlation coefficient at OS was found with U_{wind} in the North-South axis weighted
414 on 10 days ($r = 0.45$) even though it was relatively poor (Table S6). MP concentrations at BS
415 were slightly correlated with HS ($r = 0.57$) and U_{wind} in the West-East axis ($r = 0.40$), both
416 weighted on 10 days.

417 Additionally, a PCA was conducted to further explore the relationship between the
418 environmental factors and MP concentrations variability over one year (Fig. 5). Environmental
419 data weighted over the 10 days before the sampling were used as this time range provided the
420 best representation of MP concentration variance over a year. The two first dimensions account
421 for 71.3% of the total variance (PC1: 49.8%, PC2: 21.5%). The analysis represented correctly
422 the MS and OS variance, as their arrows were close to the correlation circle. BS representation
423 by studied factors was lower than for the two other stations. Weighted HS contributed to 27.1%
424 of the total variance in the first dimension, MP concentration at MS account for 22.8% and
425 weighted U_{wind} in the West-East axis to 19.1%. PC1 indicates that HS and westward winds prior

426 to the sampling increased together with the MP concentrations at MS. This trend was also shown
427 for BS but to a lesser extent. MP concentrations at MS and BS were correlated together, and
428 were also correlated to the river daily flow weighted on 10 days. Concentrations at OS
429 contributed at 50.7% of the PC2 and U_{wind} from the North-South axis accounted for 28.9%. MP
430 concentrations at the OS were increasing meanwhile northward winds increased too.

431

432 **Discussion**

433

434 4.1 Characterization and spatial distribution of beached microplastics

435 Considering morphometric data (i.e. dimensions, color and shape), the three sites (OS, MS,
436 and BS) presented a statistically similar profile of contamination. This homogeneity between
437 sites may be explained by the high proportions of pellets at each site. In previous studies, high
438 proportions of pellets already steer the morphometric data (Antunes et al., 2018; Prata et al.,
439 2020). Indeed, pellets are raw material that are calibrated at the production step so they are
440 relatively homogenous, even if different pre-production pellet types existed (e.g. 5 mm diameter
441 transparent and white, opaque and black, 3 mm of diameter red and opaque, 2 mm diameter
442 cylindrical transparent and white). These pre-production pellets were found in coastal areas
443 over the five continents, for example in California (United-States), Borneo (Malaysia), Sicilia
444 (Italy) or Jakarta (Indonesia) (Ogata et al., 2009). As a matter of fact, pellets are discarded in
445 the environment before being transformed by manufacturer, which means before being turned
446 into any kind of goods. Several studies reported that pellets represented more than 70% of
447 collected items on beaches in Portugal (Antunes et al., 2018; Prata et al., 2020) and slightly less
448 at an island off the Brazilian coast (60%, Ivar do Sul et al., 2009). Similar pellets proportions
449 (49% in this study) were detected in South Africa (Ryan et al., 2018) and at Famara beach in
450 Canary Island (Spain, Herrera et al., 2018).

451 Pellets are considered as primary MP as they are produced at a size inferior to 5 mm
452 (GESAMP, 2015). Description of MP shape is important because it can be linked, among other
453 things, to a primary or a secondary origin. In this study, primary MP (i.e. pellets only)
454 represented 49% of all the collected items (Table S4.). This result highlights the non-negligible
455 contribution of MP coming from industrial activities (e.g. production or molding). Actually,
456 plastic industries have already been suspected to be a source of pellets deposition onto beaches
457 close to industrial center. It is due to losses during several processes such as the handling of
458 pellets, the loading/unloading on and from truck or ships (Turra et al., 2015), but also at many
459 other steps like transport or cleaning (Cole and Sherrington, 2016). Port facilities are also
460 suggested as an input source of pellets in the marine environment (Antunes et al., 2018).
461 However, port facilities in the Arcachon Bay do not support commercialization and transport of
462 goods supplies. Main activities are related to local fishing, aquaculture or recreational uses. Yet,
463 Arcachon Bay is close to Bordeaux city (approximately 50 Km) and to the mouth of the Gironde
464 estuary (approximately 100 Km). Moreover, two cities (Bordeaux and Royan) are located at the
465 water's edge of the Gironde estuary. These two cities host plastic industries and/or port facilities
466 that support commercial exchanges. Thus, the Gironde estuary may catch accidentally
467 discharged and spilled pellets that may then enter the Atlantic Ocean. This estuary is one of the
468 largest in Europe and its mean flow is around $841 \text{ m}^3 \cdot \text{s}^{-1}$ (based on the annual mean flow of the
469 two main tributaries, the Garonne and Dordogne rivers, calculated over 109 and 26 years
470 respectively; <http://www.hydro.eaufrance.fr/>, last visit on April 7th 2021). Its plumes can extend
471 along the coast when southwesterly winds blow (Costoya et al., 2017). Therefore, it could be a
472 contributor to MP transport to the ocean and to the Arcachon Bay. This is further discussed in
473 Section 4.2 by analyzing the mean currents in the continental shelf area of the bay.

474 Regarding other type of shapes, fragments represented almost 40 % of all sampled particles
475 (Table S4), which was similar to proportions found in South Africa coastline (33%, Ryan et al.,

476 2018). However, higher proportions of fragments were recorded in Chile, (89 %, Hidalgo-Ruz
477 and Thiel, 2013) or in Brazil (96% in Costa et al., 2010; 99% in Pinheiro et al., 2019). Different
478 sources and pathways of contamination may lead to different shape proportions between areas.
479 However, pellets and fragments are the two predominant MP shapes in beach samples (e.g. all
480 above-cited sources). Foams are regularly found among beach litter (e.g. Antunes et al., 2018;
481 Ryan et al., 2018) and in this study they were found at each site even though it was in moderate
482 proportions (less than 30 %). Styrofoam®, which is a branded polystyrene foam, may be
483 encountered in very high proportions in some sandy beaches such as in South Korea where they
484 composed 90% of collected items (Heo et al., 2013; Kim et al., 2015). Thus, this high proportion
485 was related to the Styrofoam® buoys placed in sea farm using hanging-culture. However, we
486 have to underline that comparisons with other studies are not easy regarding the diversity of
487 size range studied (i.e. MP, mesoplastic, macroplastic), the selected sampling strategies (position
488 on the beach, sampling depth, number of replicate, etc.) or analytical methodologies (sieving,
489 density separation, etc.).

490 The low film occurrence found at OS and MS at the Arcachon Bay may be explained by an
491 easier dispersion once they are deposited on beaches. They are more likely to be dispersed by
492 wind or small perturbations than other shapes since they are thin and light. The higher
493 proportion found at BS may be due to the higher load of organic matter in the high tide line at
494 this site, which favors the retention of films. The lower occurrence of films at OS can be also
495 due to their dynamical behavior. As demonstrated by Forsberg et al., 2020, films tend to sink
496 more often in the surf zone. Additionally, McDermid and McMullen, 2004 suggested that in
497 marine environments, films and foams sank more easily due to biofilm formation on their large
498 surface and therefore, did not reach the coastline.

499

500 As mentioned above, the comparison between studies and regions should be made with
501 caution. Other than the already mentioned differences in methodology, previous studies used
502 different units regarding MP concentration description and do not systematically analyze the
503 chemical structure of sampled items, or a very small fraction (e.g. McDermid and McMullen,
504 2004; Pinheiro et al., 2019). Data from studies cited for comparison purpose included a size
505 range of particles from 63 μm (Constant et al., 2019) to 50 mm (Heo et al., 2013), and the
506 sampling depth ranged from the surface of the sand (Kusui and Noda, 2003) to first meter (Turra
507 et al., 2014). The wide range of methodologies employed in plastic pollution research field
508 make comparisons harder. When it was possible, data that better fit with our study were chosen
509 preferentially (e.g. item size range, sampling depth). Nevertheless, concentrations found at the
510 Arcachon Bay ($13.5 \pm 27.4 \text{ MP.m}^{-2}$ for the whole studied area, Table 1) were generally low
511 compared to concentrations commonly described in other sandy beaches. For instance, very
512 highly contaminated areas such as South Korea beaches displayed concentration up to $46,334$
513 $\pm 71,291 \text{ items.m}^{-2}$ (Kim et al., 2015) whereas dimly contaminated areas displayed
514 concentrations around few items per square meter like in Japanese beaches (3.41 item.m^{-2} ,
515 Kusui and Noda, 2003).

516

517 Regarding polymer types, PE is the most produced plastic type in the world
518 (PlasticsEurope, 2020). Thus, considering the whole studied area, its high prevalence (69%)
519 was not surprising. Similar proportions were reported from samples collected on beaches in
520 Brazil (78%, Turra et al., 2015), in Portugal (68%, Prata et al., 2020), or in the high tide line of
521 a touristic beach in India (52%; Karthik et al., 2018). Regarding PP, even if it is a commonly
522 produced polymer, it was identified at 17% in this study, which is close to the study made in
523 Brazil (18%, Turra et al., 2015). As reviewed by Mendoza et al. (2020), PE and PP tend to be
524 the two main polymers found in beach compartment from the Bay of Biscay (North-East

525 Atlantic Ocean), which is consistent with this study. Furthermore, PS represented here 10%,
526 which is higher than in Portugal (2%, Prata et al., 2020) or in Brazil (0%, Turra et al., 2015).
527 PE, PP and PS are mainly used in the packaging industry (PlasticsEurope, 2020) and they are
528 also the more common plastic types found on worldwide beaches (Bancin et al., 2019; De-la-
529 Torre et al., 2020; Ilechukwu et al., 2019; Karthik et al., 2018). Two other polymers, EVA and
530 PiBMA, were also found at MS in a very low proportion (around 1% of all analyzed particles).
531 As this station displayed a higher abundance of particles, the probability to find unusual
532 polymers was more important.

533 Almost all types of polymers identified in this study have a density lower than the
534 density of seawater. It means that these polymers are likely to float at the sea surface, if they
535 are not too degraded or too colonized. As demonstrated in experimental simulations (Forsberg
536 et al., 2020), these low-density particles can easily reach the coast and be deposited on the beach
537 with tides and waves.

538

539 4.2 Influence of environmental factors on microplastic beaching

540 Two contrasted environmental conditions were described in 2019, one revealing a high-
541 energy state (i.e. from October to April) and the other describing a low-energy state (i.e. from
542 May to September; Fig. 4). Higher concentrations of beached MP were mostly recovered during
543 the energetic state, concurrently with high wind speed, wave height and river daily flow. This
544 result is in agreement with previous studies on beaches from the East Atlantic coast (Portugal
545 and Canary Island) that showed higher MP concentration in winter and autumn (Antunes et al.,
546 2018; Herrera et al., 2018; Prata et al., 2020). On the contrary, during spring and summer, when
547 wind was weak wave height was low and river discharges also, MP concentrations were
548 generally lower than in winter/autumn and even presented several null concentrations. For

549 instance, in September no MP was found on any beaches when wind was particularly weak for
550 several weeks before the sampling.

551 Among the studied environmental factors, wind direction and speed stand out as key
552 factors on MP beaching at the studied sites. Looking only at one season (e.g. winter), MP
553 concentrations were higher during onshore (westerly) strong wind events (February) while
554 lower concentrations were observed during offshore (easterly) weak wind events, particularly
555 at MS and BS. The PCA analysis (Fig. 5) also highlighted the correlation of West-East winds
556 axis and monthly MP concentration at MS and BS. Indeed, seaward winds increase the inflow
557 by the South channel (Salles et al., 2015), where MS is located, so higher marine input passed
558 into the bay. This may have increased the availability of MP at sea surface and thus enhanced
559 the beaching. Onshore winds also increase the water confinement of the southeastern part of
560 the bay (IFREMER, 2007), where BS is located, which could favor the MP accumulation and
561 beaching in this region. On the contrary, offshore winds could have pushed back MP that were
562 at the sea surface close to the coastline, making the beaching harder. This behavior was already
563 demonstrated under laboratory experimental conditions (Forsberg et al., 2020). Furthermore, it
564 has been shown that offshore winds reduce the input flow of the South pass (Salles et al., 2015),
565 which may reduce the MP input into the bay and therefore beaching.

566 MP concentrations were also well correlated with significant wave height (HS) at MS and
567 BS, which are not directly exposed to waves. This may be due to the covariance of wave
568 characteristics with wind, which seems to be a prevailing driver of MP beaching at these inner
569 stations. Nevertheless, strong waves can also favor the transport of MP toward the coastline and
570 the bay entry through the Stokes drift (Forsberg et al., 2020) which can also explain the higher
571 correlation between HS and concentration of beached MP in the inner bay. OS displayed the
572 lowest MP concentrations (1.8 ± 2.4 MP per m^2 in average) which, curiously, presented a poor
573 correlation with wind and waves characteristics despite the higher exposition of this site to these

574 two factors. Actually, this high exposition to wind may explain this result given that strong
575 onshore wind events may have dispersed microplastic toward the top of the beach before the
576 sampling, as already suggested for low density microplastics by Browne et al. (2010). This may
577 lead to an underestimation of overall MP abundance at this site, and more particularly for lighter
578 MP such as polystyrene foam or other items with large surface such as films.

579

580 In addition to the environmental factors directly related to beaching, other forcing and
581 hydrodynamic processes may influence the spatial and temporal variability of MP
582 concentrations in the studied sites. In fact, flood times matched with high beaching
583 concentrations, particularly at the mouth station and a good correlation between MP
584 concentrations with river flow was found at MS and BS. The relationship between MP
585 concentrations and river discharges close to beaches was also found by Karthik et al. (2018).
586 This environmental factor cannot be directly linked to the MP beaching process but it may result
587 in a more important input of MP in the system. However, the fate of MP released at the Leyre
588 outlet will be analyzed in future modeling studies. Tidal currents and bay circulation can also
589 affect the spatial variability. Indeed, the local water mass at BS is rapidly renewed (less than 1
590 day; Plus et al., 2009), which may mitigate an accumulation effect at this region. The higher
591 concentration at MS (36.0 ± 39.2 MP.m⁻² in average) may be explained by its location at the
592 Southern Chanel and its exposition to predominant winds. This part of the bay, close to the
593 mouth, is characterized by stronger tidal currents and high residual fluxes (Plus et al., 2009)
594 that may form a privileged crossroad of debris, promoting high beaching rates during favorable
595 winds.

596 Embayment and oceanic circulation may thus influence the amount of MP that enters and
597 leaves the lagoon and thus may impact the concentrations of MP that beached around the bay.
598 The analysis of currents at the bay scale requires high-resolution numerical modeling. Here, we

599 discussed the ocean circulation at the continental shelf from the available Modeling and
600 Analysis for Coastal Research (MARC) product. We compared the average residuals current
601 velocities of the ten previous days of each sampling time point (February and May scenarios
602 are provided in Fig. S4). In general, longshore drift was oriented from North to South (see
603 February scenario in Fig. S4). However, opposite directions of currents were found in March
604 and October, while there was no clear trend in May. This North-South predominant orientation
605 of longshore drift may favor the transport of particles from the Gironde estuary to the water
606 around the bay, supporting the hypothesis discussed in Section 4.1. This hypothesis will be
607 tested in future studies together with the influence of the inner-bay currents on the MP transport
608 thanks to high-resolution numerical modeling.

609

610 Understanding and assessing the individual role and importance of environmental factors
611 on MP beaching is therefore a difficult task, especially in a coastal bay subject to multiple and
612 complex hydrodynamic processes. The fact that the different forcing followed a similar seasonal
613 variability makes this evaluation even harder. Yet, this study gives some interesting insights
614 into the influence of local hydrodynamic on MP beaching in a semi-enclosed mesotidal lagoon.
615 Wind, waves and currents seem to be important factors for understanding MP transport and
616 beaching in the different part of the bay. In particular, as MS and BS are protected from swell
617 and exposed to onshore winds, it suggests that wind orientation and speed are key factor
618 influencing beaching at these sites.

619 However, the above correlations, and therefore the influence of individual factors, should
620 be interpreted with cautious as wind, waves and river flow, respond to the similar large-scale
621 atmospheric forcings (Castelle et al., 2017; Jalón-Rojas and Castelle, 2021), displaying a similar
622 variability. An evaluation of the relative influence of each factor requires a longer discussion,
623 which considers the particular location, characteristics and conditions of each studied site, and

624 a numerical modeling study. Therefore, it will be explored in future studies by coupling two
625 numerical models, TrackMPD (Jalón-Rojas et al., 2019b) which describes MP transport in the
626 marine environment and Mars3D, that describes the hydrodynamic of the region (Kombiadou
627 et al., 2014; Lazure and Dumas, 2008).

628

629 **Conclusion**

630 In this study, the spatial and temporal variability of MP that washed up with the high tide
631 on three sandy beaches were studied for a semi-enclosed mesotidal embayment (Arcachon Bay,
632 France). MP sizes, shapes and colors were similar between the three studied sites even though
633 it could be due to the great proportion of pre-production pellets, which are calibrated MP.
634 Industrial pellets are pervasive and induce a keen interest at worldwide scale, especially because
635 of their known origin. Here, pellets represented almost the half of collected items, before
636 fragment and foam. Even though comparisons between studies are still difficult, the highest
637 concentration found at MS, were in the range of those recorded on the Northeastern part of the
638 Atlantic coast. However, mean MP concentration at the Arcachon Bay is lower compared to
639 concentrations found along the Atlantic coast and at worldwide scale.

640 Spatial and temporal distributions were analyzed together with environmental factors to
641 better understand their variability. The studied year can be divided into high and low energy
642 periods according to the strength of environmental factors, mainly wave height, wind
643 orientation and wind speed. These two high and low energy states correspond respectively to
644 high and low MP beaching displaying a marked seasonal variability. This trend was particularly
645 perceptible at MS, exposed to western winds (onshore wind) and protected from swell,
646 suggesting that wind is a key factor influencing beaching. However, other environmental and
647 hydrodynamic forcing like oceanic circulation and wave Stokes drift, river and estuarine plums,

648 water renewal from the bay or beach specific factors might also affect the presence of particles
649 at nearshore waters and beaching.

650 Beaches are areas of great interest in the description of MP distribution. Actually, MP fluxes
651 and budget among aquatic compartments remain unknown and beaches tend to be a hot spot
652 for plastic deposition (in particular at the tide lines). Due to multiple different MP characteristics
653 (e.g. morphological or chemical), the description of their transport and behavior is still complex.
654 Additionally, many environmental and anthropic factors tend to play a role in this process.
655 Therefore, it is not possible for now to generalize the importance of each factor at the global
656 scale since no clear pattern is reported in the literature and there are important variations at local
657 scale. To model complex processes such as beaching and recapturing of MP on beaches, we
658 need to document their distribution at different locations and scales but also at different times.
659 We also need to study sites where multiple environmental and anthropic drivers could be taken
660 into account both individually and in combination. To collect far more data, citizen sciences
661 have been shown to be useful as demonstrated for instance by Hidalgo-Ruz and Thiel (2013)
662 and encouraged by the Marine Strategy Framework Directive (2013). The protocol described
663 in this study, along with some documentation helping recognize MP and the high tide line, can
664 be used for citizen science and NGO awareness activities as it has already been tested in the
665 Atlantic coastline during this project.

666

667

668 Author contributions

669 This study was conceptualized by BM, JC, SL and CL. Methodologies were set up by BM, JC,
670 SL, IJR and CL. Data validation and duration was made by IJR. MP sampling and
671 characterization (both visual and chemical), statistical analysis and visualization were made by
672 CL. Environmental factors analysis and visualizations were made by IJR, JL and CL. Resources

673 were provided by SV, JC, SL and BM. CL and IJR wrote the original draft and IJR, SV, JC, SL,
674 and BM reviewed and edited the manuscript. JC, SL, BM and SV supervised CL. BM, JC and
675 SL acquired the financial support and BM managed the project. All authors contributed to the
676 article and approved the submitted version.

677

678 Acknowledgements

679 The authors want to thanks Bruno Castelle from the UMR EPOC for providing and calibrating
680 swell coming from HOMERE database (Laboratory for Ocean Physics and Satellite remote
681 sensing and *Laboratoire Comportement des structures en Mer*). We thanks the French national
682 meteorological service (*Météo France*) for providing wind data and the *Banque Hydro* support
683 by the French ministry of ecological transition for river flow and the French Research Institute
684 for Exploitation of the Sea (IFREMER) for providing current data by the way of the MARS
685 model. We also thanks Florane Le Bihanic, Quentin Perdriat and Gabriel Rampazzo Magalhães
686 for their help in sampling and Jeyan Bichon for her contribution in ATR-FTIR analysis.

687

688

689

690 Fundings

691 This study was conducted in the frame of the ARPLASTIC research project. This work was
692 funded by the Nouvelle-Aquitaine French region, the Water council *Agence de l'eau Adour-*
693 *Garonne*, the local inter-city board *Syndicat Intercommunal du Bassin d'Arcachon* and the local
694 marine national park *Parc National Marin du Bassin d'Arcachon (Office Français de la*
695 *Biodiversité)*.

696

697 Figure 1. A) Localization of the Arcachon Bay, the studied stations (OS : Outside Station,
698 MS :Mouth Station, BS: Back Station), the anemometer, the tide gauge and the Wharf sewage.

699 B) Sketch of the sampling protocol _ Sizing: 1.5 column

700

701

702 Figure 2. Morphological and chemical distribution of MP among studied sites: A) Shape of
703 visually characterized particles, B) Polymer types of chemically identified particles.

704 Polyethylene (PE), polypropylene (PP), polystyrene (PS), ethyl vinyl acetate (EVA),

705 poly(isobutyl methacrylate) (PiBMA), non-plastic (NP) and unknown polymer (UNK).

706 Detailed percentages can be found in text or in Table S4 _ Sizing: 1.5 column

707

708

709 Figure 3. Box plot of MP concentration for each sampling station (the middle line represents

710 the median value and the red rhombus represent the average concentration). Paired comparisons

711 between sites performed with the W-test are shown by the thicker black lines (ns: non-

712 significant, ** p-values <0.01). _ Sizing: 1 column

713

714

715 Figure 4. Temporal variations of A) MP concentration at each site (when no data is shown it

716 means that concentration was 0 MP.m⁻²), B) tidal range (TR, in m), C) significant wave height

717 (HS, in m), D) wind speed and direction (speed : U_{wind} in m¹.s⁻¹; for wind orientation see wind

718 rose) and E) mean daily flow of the Leyre river (Q, in m³.s⁻¹). Data from December 1st 2018 to

719 December 31st 2019. _ Sizing : 1.5 column

720

721

722 Figure 5. PCA variable plot based on monthly data. All environmental factors are weighted over
723 the 10 days before the sampling. OS: MP concentration at the Outside Station; MS: MP
724 concentration at the Mouth Station; BS: MP concentration at the Back Station;
725 SpeedWind_NS10d: wind speed in the North-South direction axis (+ North ; - South);
726 SpeedWind_EW10d: wind speed in the East-West direction axis (+ West ; - East);
727 HeightWave10d: significant wave height ; Flow10d: mean river daily flow. _ Sizing: 1 column

728

729 Bibliography

- 730 Amélineau, F., Bonnet, D., Heitz, O., Mortreux, V., Harding, A.M.A., Karnovsky, N., Walkusz,
731 W., Fort, J., Grémillet, D., 2016. Microplastic pollution in the Greenland Sea:
732 Background levels and selective contamination of planktivorous diving seabirds.
733 Environ. Pollut. 219, 1131–1139. <https://doi.org/10.1016/j.envpol.2016.09.017>
- 734 Andrady, A.L., 2011. Microplastics in the marine environment. Mar. Pollut. Bull. 62, 1596–
735 1605. <https://doi.org/10.1016/j.marpolbul.2011.05.030>
- 736 Antunes, J., Frias, J., Sobral, P., 2018. Microplastics on the Portuguese coast. Mar. Pollut. Bull.
737 131, 294–302. <https://doi.org/10.1016/j.marpolbul.2018.04.025>
- 738 Baak, J.E., Provencher, J.F., Mallory, M.L., 2020. Plastic ingestion by four seabird species in
739 the Canadian Arctic: Comparisons across species and time. Mar. Pollut. Bull. 158,
740 111386. <https://doi.org/10.1016/j.marpolbul.2020.111386>
- 741 Balthazar-Silva, D., Turra, A., Moreira, F.T., Camargo, R.M., Oliveira, A.L., Barbosa, L.,
742 Gorman, D., 2020. Rainfall and tidal cycle regulate seasonal inputs of microplastic
743 pellets to sandy beaches. Front. Environ. Sci. 8, 123.
744 <https://doi.org/10.3389/fenvs.2020.00123>
- 745 Bancin, L.J., Walther, B.A., Lee, Y.-C., Kunz, A., 2019. Two-dimensional distribution and
746 abundance of micro- and mesoplastic pollution in the surface sediment of Xialiao Beach,
747 New Taipei City, Taiwan. Mar. Pollut. Bull. 140, 75–85.
748 <https://doi.org/10.1016/j.marpolbul.2019.01.028>
- 749 Bergmann, M., Gutow, L., Klages, M., Alfred-Wegener-Institut, Göteborgs universitet (Eds.),
750 2015. Marine anthropogenic litter, Springer Open. Springer, Cham Heidelberg New
751 York Dordrecht London.

752 Boucher, J., Friot, D., 2017. Primary microplastics in the oceans: A global evaluation of sources.
753 IUCN International Union for Conservation of Nature.
754 <https://doi.org/10.2305/IUCN.CH.2017.01.en>

755 Boudière, E., Maisondieu, C., Ardhuin, F., Accensi, M., Pineau-Guillou, L., Lepesqueur, J.,
756 2013. A suitable metocean hindcast database for the design of Marine energy converters.
757 Int. J. Mar. Energy 3–4, e40–e52. <https://doi.org/10.1016/j.ijome.2013.11.010>

758 Browne, M.A., Crump, P., Niven, S.J., Teuten, E., Tonkin, A., Galloway, T., Thompson, R.,
759 2011. Accumulation of Microplastic on Shorelines Woldwide: Sources and Sinks.
760 Environ. Sci. Technol. 45, 9175–9179. <https://doi.org/10.1021/es201811s>

761 Browne, M.A., Galloway, T.S., Thompson, R.C., 2010. Spatial Patterns of Plastic Debris along
762 Estuarine Shorelines. Environ. Sci. Technol. 44, 3404–3409.
763 <https://doi.org/10.1021/es903784e>

764 Carvalho, J.P.S., Silva, T.S., Costa, M.F., 2021. Distribution, characteristics and short-term
765 variability of microplastics in beach sediment of Fernando de Noronha Archipelago,
766 Brazil. Mar. Pollut. Bull. 166, 112212. <https://doi.org/10.1016/j.marpolbul.2021.112212>

767 Castelle, B., Bonneton, P., Dupuis, H., Sénéchal, N., 2007. Double bar beach dynamics on the
768 high-energy meso-macrotidal French Aquitanian Coast: A review. Mar. Geol. 245, 141–
769 159. <https://doi.org/10.1016/j.margeo.2007.06.001>

770 Castelle, B., Bujan, S., Marieu, V., Ferreira, S., 2020. 16 years of topographic surveys of rip-
771 channelled high-energy meso-macrotidal sandy beach. Sci. Data 7, 410.
772 <https://doi.org/10.1038/s41597-020-00750-5>

773 Castelle, B., Dodet, G., Masselink, G., Scott, T., 2017. A new climate index controlling winter
774 wave activity along the Atlantic coast of Europe: The West Europe Pressure Anomaly.
775 Geophys. Res. Lett. 44, 1384–1392. <https://doi.org/10.1002/2016GL072379>

776 Castelle, B., Marieu, V., Bujan, S., Ferreira, S., Parisot, J.-P., Capo, S., Sénéchal, N.,
777 Chouzenoux, T., 2014. Equilibrium shoreline modelling of a high-energy meso-
778 macrotidal multiple-barred beach. *Mar. Geol.* 347, 85–94.
779 <https://doi.org/10.1016/j.margeo.2013.11.003>

780 Cayocca, F., 2001. Long-term morphological modeling of a tidal inlet: the Arcachon Basin,
781 France. *Coast. Eng.* 42, 115–142. [https://doi.org/doi:10.1016/S0378-3839\(00\)00053-3](https://doi.org/doi:10.1016/S0378-3839(00)00053-3).

782 Cole, G., Sherrington, C., 2016. Study to quantify pellet emissions in the UK 45.

783 Cole, M., Lindeque, P., Halsband, C., Galloway, T.S., 2011. Microplastics as contaminants in
784 the marine environment: A review. *Mar. Pollut. Bull.* 62, 2588–2597.
785 <https://doi.org/10.1016/j.marpolbul.2011.09.025>

786 Constant, M., Kerhervé, P., Mino-Vercellio-Verollet, M., Dumontier, M., Sánchez Vidal, A.,
787 Canals, M., Heussner, S., 2019. Beached microplastics in the Northwestern
788 Mediterranean Sea. *Mar. Pollut. Bull.* 142, 263–273.
789 <https://doi.org/10.1016/j.marpolbul.2019.03.032>

790 Cooper, D.A., Corcoran, P.L., 2010. Effects of mechanical and chemical processes on the
791 degradation of plastic beach debris on the island of Kauai, Hawaii. *Mar. Pollut. Bull.* 60,
792 650–654. <https://doi.org/10.1016/j.marpolbul.2009.12.026>

793 Corcoran, P.L., Biesinger, M.C., Grifi, M., 2009. Plastics and beaches: A degrading relationship.
794 *Mar. Pollut. Bull.* 58, 80–84. <https://doi.org/10.1016/j.marpolbul.2008.08.022>

795 Cormier, B., Gambardella, C., Tato, T., Perdriat, Q., Costa, E., Veclin, C., Le Bihanic, F., Grassl,
796 B., Dubocq, F., Kärman, A., Van Arkel, K., Lemoine, S., Lagarde, F., Morin, B.,
797 Garaventa, F., Faimali, M., Cousin, X., Bégout, M.-L., Beiras, R., Cachot, J., 2021.
798 Chemicals sorbed to environmental microplastics are toxic to early life stages of aquatic
799 organisms. *Ecotoxicol. Environ. Saf.* 208, 111665.
800 <https://doi.org/10.1016/j.ecoenv.2020.111665>

801 Costa, M.F., Ivar do Sul, J.A., Silva-Cavalcanti, J.S., Araújo, M.C.B., Spengler, Â., Tourinho,
802 P.S., 2010. On the importance of size of plastic fragments and pellets on the strandline:
803 a snapshot of a Brazilian beach. *Environ. Monit. Assess.* 168, 299–304.
804 <https://doi.org/10.1007/s10661-009-1113-4>

805 Costoya, X., Fernández-Nóvoa, D., deCastro, M., Gómez-Gesteira, M., 2017. Loire and
806 Gironde turbid plumes: Characterization and influence on thermohaline properties. *J.*
807 *Sea Res.* 130, 7–16. <https://doi.org/10.1016/j.seares.2017.04.003>

808 Courtene-Jones, W., Quinn, B., Ewins, C., Gary, S.F., Narayanaswamy, B.E., 2019. Consistent
809 microplastic ingestion by deep-sea invertebrates over the last four decades (1976–2015),
810 a study from the North East Atlantic. *Environ. Pollut.* 244, 503–512.
811 <https://doi.org/10.1016/j.envpol.2018.10.090>

812 Cousin, X., Batel, A., Bringer, A., Hess, S., Bégout, M.-L., Braunbeck, T., 2020. Microplastics
813 and sorbed contaminants – Trophic exposure in fish sensitive early life stages. *Mar.*
814 *Environ. Res.* 161, 105126. <https://doi.org/10.1016/j.marenvres.2020.105126>

815 da Costa, J.P., Santos, P.S.M., Duarte, A.C., Rocha-Santos, T., 2016. (Nano)plastics in the
816 environment – Sources, fates and effects. *Sci. Total Environ.* 566–567, 15–26.
817 <https://doi.org/10.1016/j.scitotenv.2016.05.041>

818 Davidson, M.A., Splinter, K.D., Turner, I.L., 2013. A simple equilibrium model for predicting
819 shoreline change. *Coast. Eng.* 73, 191–202.
820 <https://doi.org/10.1016/j.coastaleng.2012.11.002>

821 De-la-Torre, G.E., Dioses-Salinas, D.C., Castro, J.M., Antay, R., Fernández, N.Y., Espinoza-
822 Morriberón, D., Saldaña-Serrano, M., 2020. Abundance and distribution of
823 microplastics on sandy beaches of Lima, Peru. *Mar. Pollut. Bull.* 151, 110877.
824 <https://doi.org/10.1016/j.marpolbul.2019.110877>

825 Engler, R.E., 2012. The complex interaction between marine debris and toxic chemicals in the
826 ocean. *Environ. Sci. Technol.* 46, 12302–12315. <https://doi.org/10.1021/es3027105>

827 Eriksen, M., Lebreton, L.C.M., Carson, H.S., Thiel, M., Moore, C.J., Borerro, J.C., Galgani, F.,
828 Ryan, P.G., Reisser, J., 2014. Plastic pollution in the world's oceans: More than 5 trillion
829 plastic pieces weighing over 250,000 tons afloat at sea. *PLoS ONE* 9, e111913.
830 <https://doi.org/10.1371/journal.pone.0111913>

831 Fok, L., Cheung, P.K., 2015. Hong Kong at the Pearl River Estuary: A hotspot of microplastic
832 pollution. *Mar. Pollut. Bull.* 99, 112–118.
833 <https://doi.org/10.1016/j.marpolbul.2015.07.050>

834 Forsberg, P.L., Sous, D., Stocchino, A., Chemin, R., 2020. Behaviour of plastic litter in
835 nearshore waters: First insights from wind and wave laboratory experiments. *Mar. Pollut.*
836 *Bull.* 153, 111023. <https://doi.org/10.1016/j.marpolbul.2020.111023>

837 Frias, J.P.G.L., Nash, R., 2019. Microplastics: Finding a consensus on the definition. *Mar. Pollut.*
838 *Bull.* 138, 145–147. <https://doi.org/10.1016/j.marpolbul.2018.11.022>

839 Gago, J., Galgani, F., Maes, T., Thompson, R.C., 2016. Microplastics in seawater:
840 Recommendations from the Marine Strategy Framework Directive Implementation
841 Process. *Front. Mar. Sci.* 3. <https://doi.org/10.3389/fmars.2016.00219>

842 GESAMP, 2015. Sources, fate and effects of microplastics in the marine environment: a global
843 assessment.

844 Geyer, R., Jambeck, J.R., Law, K.L., 2017. Production, use, and fate of all plastics ever made.
845 *Sci. Adv.* 3, e1700782. <https://doi.org/10.1126/sciadv.1700782>

846 Gorman, D., Moreira, F.T., Turra, A., Fontenelle, F.R., Combi, T., Bicego, M.C., de Castro
847 Martins, C., 2019. Organic contamination of beached plastic pellets in the South Atlantic:
848 Risk assessments can benefit by considering spatial gradients. *Chemosphere* 223, 608–
849 615. <https://doi.org/10.1016/j.chemosphere.2019.02.094>

850 Govere, T., United Nations, Environment Programme, Division of Early Warning and
851 Assessment, 2014. UNEP year book 2014 emerging issues in our global environment.
852 United Nations Environment Programme (UNEP), Nairobi.

853 Heo, N.W., Hong, S.H., Han, G.M., Hong, S., Lee, J., Song, Y.K., Jang, M., Shim, W.J., 2013.
854 Distribution of small plastic debris in cross-section and high strandline on Heungnam
855 beach, South Korea. *Ocean Sci. J.* 48, 225–233. [https://doi.org/10.1007/s12601-013-](https://doi.org/10.1007/s12601-013-0019-9)
856 [0019-9](https://doi.org/10.1007/s12601-013-0019-9)

857 Herrera, A., Asensio, M., Martínez, I., Santana, A., Packard, T., Gómez, M., 2018. Microplastic
858 and tar pollution on three Canary Islands beaches: An annual study. *Mar. Pollut. Bull.*
859 129, 494–502. <https://doi.org/10.1016/j.marpolbul.2017.10.020>

860 Hidalgo-Ruz, V., Gutow, L., Thompson, R.C., Thiel, M., 2012. Microplastics in the Marine
861 Environment: A review of the methods used for identification and quantification.
862 *Environ. Sci. Technol.* 46, 3060–3075. <https://doi.org/10.1021/es2031505>

863 Hidalgo-Ruz, V., Thiel, M., 2013. Distribution and abundance of small plastic debris on beaches
864 in the SE Pacific (Chile): A study supported by a citizen science project. *Mar. Environ.*
865 *Res.* 87–88, 12–18. <https://doi.org/10.1016/j.marenvres.2013.02.015>

866 IFREMER, 2007. Caractérisation des composantes hydrodynamiques d'une lagune mésotidale,
867 le Bassin d'Arcachon 54.

868 Ilechukwu, I., Ndukwe, G.I., Mgbemena, N.M., Akandu, A.U., 2019. Occurrence of
869 microplastics in surface sediments of beaches in Lagos, Nigeria. *Eur. Chem. Bull.* 8, 371.
870 <https://doi.org/10.17628/ecb.2019.8.371-375>

871 Ivar do Sul, J.A., Spengler, Â., Costa, M.F., 2009. Here, there and everywhere. Small plastic
872 fragments and pellets on beaches of Fernando de Noronha (Equatorial Western Atlantic).
873 *Mar. Pollut. Bull.* 58, 1236–1238. <https://doi.org/10.1016/j.marpolbul.2009.05.004>

874 Jalón-Rojas, I., Castelle, B., 2021. Climate control of multidecadal variability in river discharge
875 and precipitation in Western Europe. *Water* 13, 257. <https://doi.org/10.3390/w13030257>

876 Jalón-Rojas, I., Wang, X.-H., Fredj, E., 2019a. Technical note: On the importance of a three-
877 dimensional approach for modelling the transport of neustic microplastics. *Ocean Sci.*
878 15, 717–724. <https://doi.org/10.5194/os-15-717-2019>

879 Jalón-Rojas, I., Wang, X.H., Fredj, E., 2019b. A 3D numerical model to Track Marine Plastic
880 Debris (TrackMPD): Sensitivity of microplastic trajectories and fates to particle
881 dynamical properties and physical processes. *Mar. Pollut. Bull.* 141, 256–272.
882 <https://doi.org/10.1016/j.marpolbul.2019.02.052>

883 Jeftic, L., Sheavly, S.B., Adler, E., Meith, N., 2009. Marine litter: a global challenge. Regional
884 Seas, United Nations Environment Programme, Nairobi, Kenya.

885 Karthik, R., Robin, R.S., Purvaja, R., Ganguly, D., Anandavelu, I., Raghuraman, R., Hariharan,
886 G., Ramakrishna, A., Ramesh, R., 2018. Microplastics along the beaches of southeast
887 coast of India. *Sci. Total Environ.* 645, 1388–1399.
888 <https://doi.org/10.1016/j.scitotenv.2018.07.242>

889 Kassambara, A., 2020. ggpubr: “ggplot2” Based Publication Ready Plots.

890 Kim, I.-S., Chae, D.-H., Kim, S.-K., Choi, S., Woo, S.-B., 2015. Factors influencing the spatial
891 variation of microplastics on high-tidal coastal beaches in Korea. *Arch. Environ.*
892 *Contam. Toxicol.* 69, 299–309. <https://doi.org/10.1007/s00244-015-0155-6>

893 Kombiadou, K., Ganthu, F., Verney, R., Plus, M., Sottolichio, A., 2014. Modelling the effects
894 of *Zostera noltei* meadows on sediment dynamics: application to the Arcachon lagoon.
895 *Ocean Dyn.* 64, 1499–1516. <https://doi.org/10.1007/s10236-014-0754-1>

896 Kusui, T., Noda, M., 2003. International survey on the distribution of stranded and buried litter
897 on beaches along the Sea of Japan. *Mar. Pollut. Bull.* 47, 175–179.
898 [https://doi.org/10.1016/S0025-326X\(02\)00478-2](https://doi.org/10.1016/S0025-326X(02)00478-2)

899 Lazure, P., Dumas, F., 2008. An external–internal mode coupling for a 3D hydrodynamical
900 model for applications at regional scale (MARS). *Adv. Water Resour.* 31, 233–250.
901 <https://doi.org/10.1016/j.advwatres.2007.06.010>

902 Lo, H.-S., Lee, Y.-K., Po, B.H.-K., Wong, L.-C., Xu, X., Wong, C.-F., Wong, C.-Y., Tam, N.F.-
903 Y., Cheung, S.-G., 2020. Impacts of Typhoon Mangkhut in 2018 on the deposition of
904 marine debris and microplastics on beaches in Hong Kong. *Sci. Total Environ.* 716,
905 137172. <https://doi.org/10.1016/j.scitotenv.2020.137172>

906 Lorin, J., Viguier, J., 1987. Hydrosedimentary conditions and present evolution of Aquitaine
907 Coast. *Bull Inst Bassin Aquitaine* 41, 95–108

908 Lusher, A.L., Bråte, I.L.N., Munno, K., Hurley, R.R., Welden, N.A., 2020. Is it or isn't it: the
909 importance of visual classification in microplastic characterization. *Appl. Spectrosc.* 74,
910 1139–1153. <https://doi.org/10.1177/0003702820930733>

911 Marine Strategy Framework Directive, 2013. Guidance on monitoring of marine litter in
912 European seas. Publications Office, LU.

913 Massos, A., Turner, A., 2017. Cadmium, lead and bromine in beached microplastics. *Environ.*
914 *Pollut.* 227, 139–145. <https://doi.org/10.1016/j.envpol.2017.04.034>

915 Matiddi, M., Vandeperre, F., Claro, F., Kaska, Y., Kaberi, H., Revuelta, O., Piermarini, R.,
916 Daffina, R., Pisapia, M., Genta, D., Sözbilen, D., Bradai, M.N., Rodríguez, Y.,
917 Gambaiani, D., Tsangaris, C., Chaieb, O., Moussier, J., Loza, A.L., Miaud, C., 2019.
918 Data collection on marine litter ingestion in sea turtles and thresholds for good
919 environmental status. *J. Vis. Exp.* 9.

920 McDermid, K.J., McMullen, T.L., 2004. Quantitative analysis of small-plastic debris on
921 beaches in the Hawaiian archipelago. *Mar. Pollut. Bull.* 48, 790–794.
922 <https://doi.org/10.1016/j.marpolbul.2003.10.017>

923 Mendoza, A., Osa, J.L., Basurko, O.C., Rubio, A., Santos, M., Gago, J., Galgani, F., Peña-
924 Rodriguez, C., 2020. Microplastics in the Bay of Biscay: An overview. *Mar. Pollut. Bull.*
925 153, 110996. <https://doi.org/10.1016/j.marpolbul.2020.110996>

926 Moore, C.J., 2008. Synthetic polymers in the marine environment: A rapidly increasing, long-
927 term threat. *Environ. Res.* 108, 131–139. <https://doi.org/10.1016/j.envres.2008.07.025>

928 Ogata, Y., Takada, H., Mizukawa, K., Hirai, H., Iwasa, S., Endo, S., Mato, Y., Saha, M., Okuda,
929 K., Nakashima, A., Murakami, M., Zurcher, N., Booyatumanondo, R., Zakaria, M.P.,
930 Dung, L.Q., Gordon, M., Miguez, C., Suzuki, S., Moore, C., Karapanagioti, H.K.,
931 Weerts, S., McClurg, T., Burrell, E., Smith, W., Velkenburg, M.V., Lang, J.S., Lang, R.C.,
932 Laursen, D., Danner, B., Stewardson, N., Thompson, R.C., 2009. International Pellet
933 Watch: Global monitoring of persistent organic pollutants (POPs) in coastal waters. 1.
934 Initial phase data on PCBs, DDTs, and HCHs. *Mar. Pollut. Bull.* 58, 1437–1446.
935 <https://doi.org/10.1016/j.marpolbul.2009.06.014>

936 Pannetier, P., Morin, B., Le Bihanic, F., Dubreil, L., Clérandeau, C., Chouvellon, F., Van Arkel,
937 K., Danion, M., Cachot, J., 2020. Environmental samples of microplastics induce
938 significant toxic effects in fish larvae. *Environ. Int.* 134, 105047.
939 <https://doi.org/10.1016/j.envint.2019.105047>

940 Pérez-Alvelo, K.M., Llegus, E.M., Forestier-Babilonia, J.M., Elías-Arroyo, C.V., Pagán-
941 Malavé, K.N., Bird-Rivera, G.J., Rodríguez-Sierra, C.J., 2021. Microplastic pollution
942 on sandy beaches of Puerto Rico. *Mar. Pollut. Bull.* 164, 112010.
943 <https://doi.org/10.1016/j.marpolbul.2021.112010>

944 Pineau-Guillou, L., 2013. PREVIMER. Validation des modèles hydrodynamiques 2D des
945 cÃ´tes de la Manche et de l'Atlantique (No. 26800). IFREMER,
946 ODE/DYNECO/PHYSED/2013-05.

947 Pinheiro, L.M., Monteiro, R.C.P., Ivar do Sul, J.A., Costa, M.F., 2019. Do beachrocks affect
948 microplastic deposition on the strandline of sandy beaches? *Mar. Pollut. Bull.* 141, 569–
949 572. <https://doi.org/10.1016/j.marpolbul.2019.03.010>

950 PlasticsEurope, 2020. *Plastics - the Facts 2020*.

951 Plus, M., Dumas, F., Stanisière, J.-Y., Maurer, D., 2009. Hydrodynamic characterization of the
952 Arcachon Bay, using model-derived descriptors. *Cont. Shelf Res.* 6.

953 Prata, J.C., Reis, V., Paço, A., Martins, P., Cruz, A., da Costa, J.P., Duarte, A.C., Rocha-Santos,
954 T., 2020. Effects of spatial and seasonal factors on the characteristics and carbonyl index
955 of (micro)plastics in a sandy beach in Aveiro, Portugal. *Sci. Total Environ.* 709, 135892.
956 <https://doi.org/10.1016/j.scitotenv.2019.135892>

957 Ryan, P.G., Perold, V., Osborne, A., Moloney, C.L., 2018. Consistent patterns of debris on South
958 African beaches indicate that industrial pellets and other mesoplastic items mostly
959 derive from local sources. *Environ. Pollut.* 238, 1008–1016.
960 <https://doi.org/10.1016/j.envpol.2018.02.017>

961 Salles, P., Valle-Levinson, A., Sottolichio, A., Senechal, N., 2015. Wind-driven modifications
962 to the residual circulation in an ebb-tidal delta: Arcachon Lagoon, Southwestern France.
963 *J. Geophys. Res. Oceans* 120, 728–740. <https://doi.org/10.1002/2014JC010311>

964 Scopetani, C., Cincinelli, A., Martellini, T., Lombardini, E., Ciofini, A., Fortunati, A., Pasquali,
965 V., Ciattini, S., Ugolini, A., 2018. Ingested microplastic as a two-way transporter for
966 PBDEs in *Talitrus saltator*. *Environ. Res.* 167, 411–417.
967 <https://doi.org/10.1016/j.envres.2018.07.030>

968 Sénéchal, N., Gouriou, T., Castelle, B., Parisot, J.-P., Capo, S., Bujan, S., Howa, H., 2009.
969 Morphodynamic response of a meso- to macro-tidal intermediate beach based on a long-
970 term data set. *Geomorphology* 107, 263–274.
971 <https://doi.org/10.1016/j.geomorph.2008.12.016>

972 Splinter, K.D., Turner, I.L., Davidson, M.A., 2013. How much data is enough? The importance
973 of morphological sampling interval and duration for calibration of empirical shoreline
974 models. *Coast. Eng.* 77, 14–27. <https://doi.org/10.1016/j.coastaleng.2013.02.009>

975 Tata, T., Belabed, B.E., Bououdina, M., Bellucci, S., 2020. Occurrence and characterization of
976 surface sediment microplastics and litter from North African coasts of Mediterranean
977 Sea: Preliminary research and first evidence. *Sci. Total Environ.* 713, 136664.
978 <https://doi.org/10.1016/j.scitotenv.2020.136664>

979 Thompson, R.C., Swan, S.H., Moore, C.J., vom Saal, F.S., 2009. Our plastic age. *Philos. Trans.*
980 *R. Soc. B Biol. Sci.* 364, 1973–1976. <https://doi.org/10.1098/rstb.2009.0054>

981 Turra, A., Manzano, A.B., Dias, R.J.S., Mahiques, M.M., Barbosa, L., Balthazar-Silva, D.,
982 Moreira, F.T., 2015. Three-dimensional distribution of plastic pellets in sandy beaches:
983 shifting paradigms. *Sci. Rep.* 4, 4435. <https://doi.org/10.1038/srep04435>

984 Vlachogianni, T., Fortibuoni, T., Ronchi, F., Zeri, C., Mazziotti, C., Tutman, P., Varezić, D.B.,
985 Palatinus, A., Trdan, Š., Peterlin, M., Mandić, M., Markovic, O., Prvan, M., Kaberi, H.,
986 Prevenios, M., Kolutari, J., Kroqi, G., Fusco, M., Kalampokis, E., Scoullou, M., 2018.
987 Marine litter on the beaches of the Adriatic and Ionian Seas: An assessment of their
988 abundance, composition and sources. *Mar. Pollut. Bull.* 131, 745–756.
989 <https://doi.org/10.1016/j.marpolbul.2018.05.006>

990 Wickham, H., 2016. *ggplot2: Elegant Graphics for Data Analysis*, Springer-Verlag New York.

991 Williams, A.T., Randerson, P., Allen, C., Cooper, J.A.G., 2017. Beach litter sourcing: A trawl
992 along the Northern Ireland coastline. *Mar. Pollut. Bull.* 122, 47–64.
993 <https://doi.org/10.1016/j.marpolbul.2017.05.066>

994 Williams, A.T., Randerson, P., Di Giacomo, C., Anfuso, G., Macias, A., Perales, J.A., 2016.
995 Distribution of beach litter along the coastline of Cádiz, Spain. *Mar. Pollut. Bull.* 107,
996 77–87. <https://doi.org/10.1016/j.marpolbul.2016.04.015>

997 Zhang, H., 2017. Transport of microplastics in coastal seas. *Estuar. Coast. Shelf Sci.* 199, 74–
998 86. <https://doi.org/10.1016/j.ecss.2017.09.032>

Submission N° : STOTEN-D-21-10923

Table 1. Abundance of sampled particles (visually characterized), abundance of particles analyzed by ATR-FTIR, abundance of particles that were chemically identified as MP, contribution of MP particles among all collected particles (in %), mean MP concentration and standard deviation (SD) after data correction (in MP.m⁻²) and concentrations range found at each site and in the whole studied area (Total) (in MP.m⁻²).

	Sampled particles	Particles analyzed by ATR-FTIR	Particles identified as MP	Contribution of MP (in %)	MP concentration (mean ± SD, in MP.m ⁻²)	Concentration range (in MP.m ⁻²)
OS	22	22	21	95.5	1.8 ± 2.4	0.0 – 8.0
MS	443	372	364	97.8	36.0 ± 39.2	0.0 – 113.0
BS	35	35	32	91.4	2.7 ± 4.4	0.0 – 15.0
Total	500	430	417	96.9	13.5 ± 27.4	0.0 – 113.0

Table 2. Color proportions (in %) of visually characterized particles at the three studied sites and in the whole studied area (Total)

	White	Blue	Black	Red	Orange	Grey	Green	Pink	Yellow
OS	70.0	9.9	3.8	1.8	5.4	1.3	3.2	0.5	4.1
MS	72.7	13.6	9.1	4.6	0.0	0.0	0.0	0.0	0.0
BS	45.7	28.6	5.7	5.7	0.0	5.7	5.7	0.0	2.9
Total	68.4	11.4	4.2	2.2	4.8	1.6	3.2	0.4	3.8

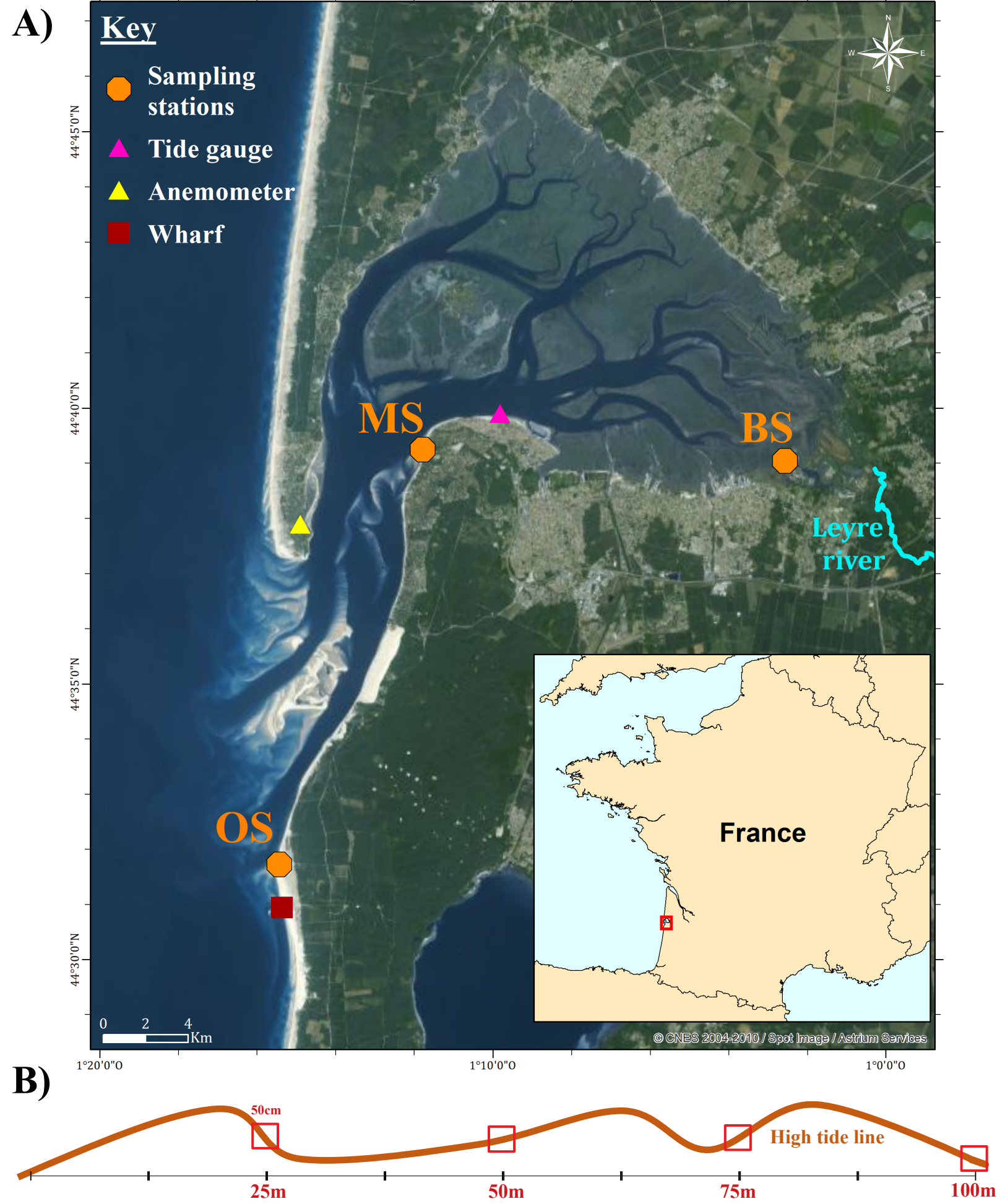


Figure **A)** Shapes Pellet Fragment Foam Films Filament

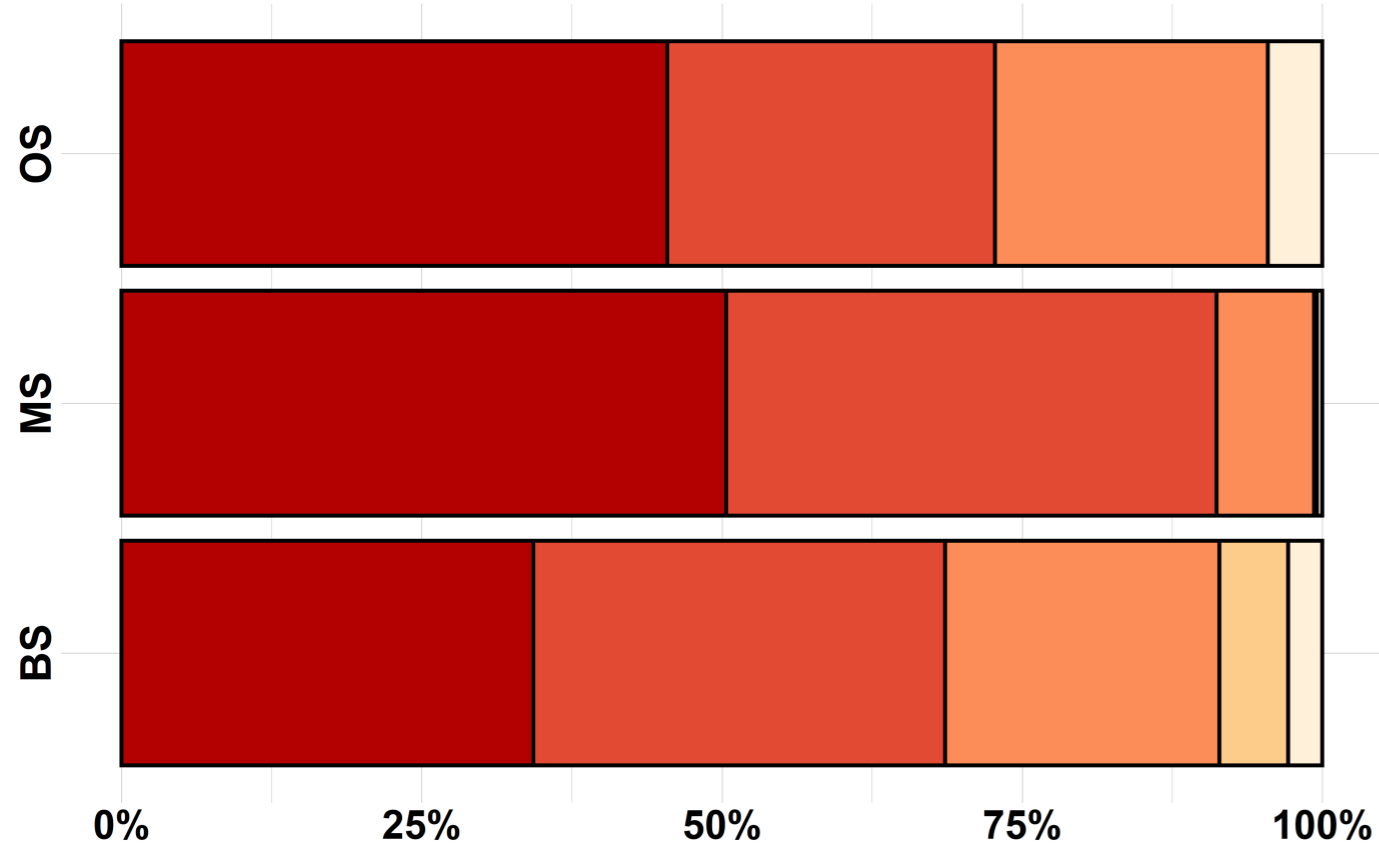
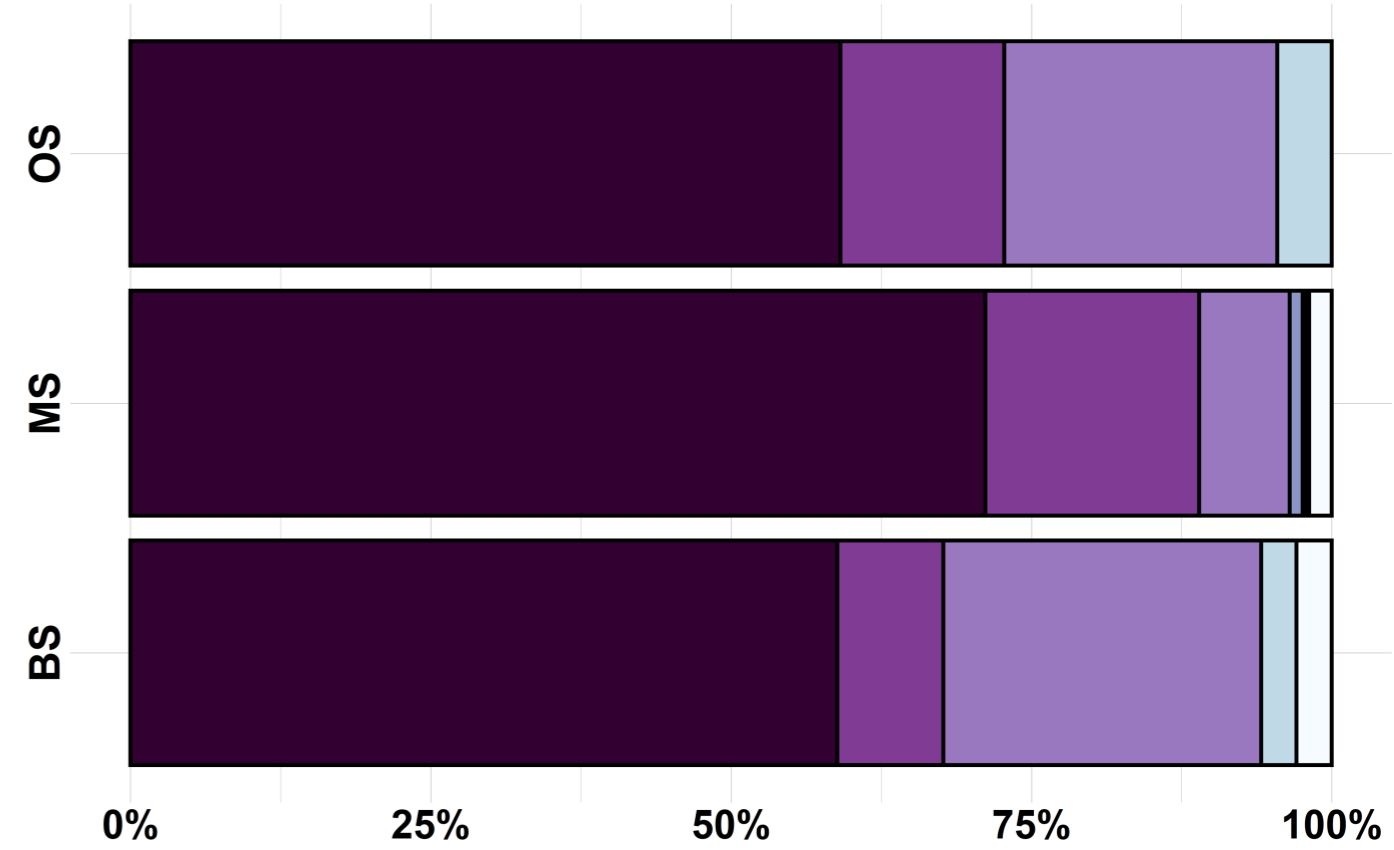
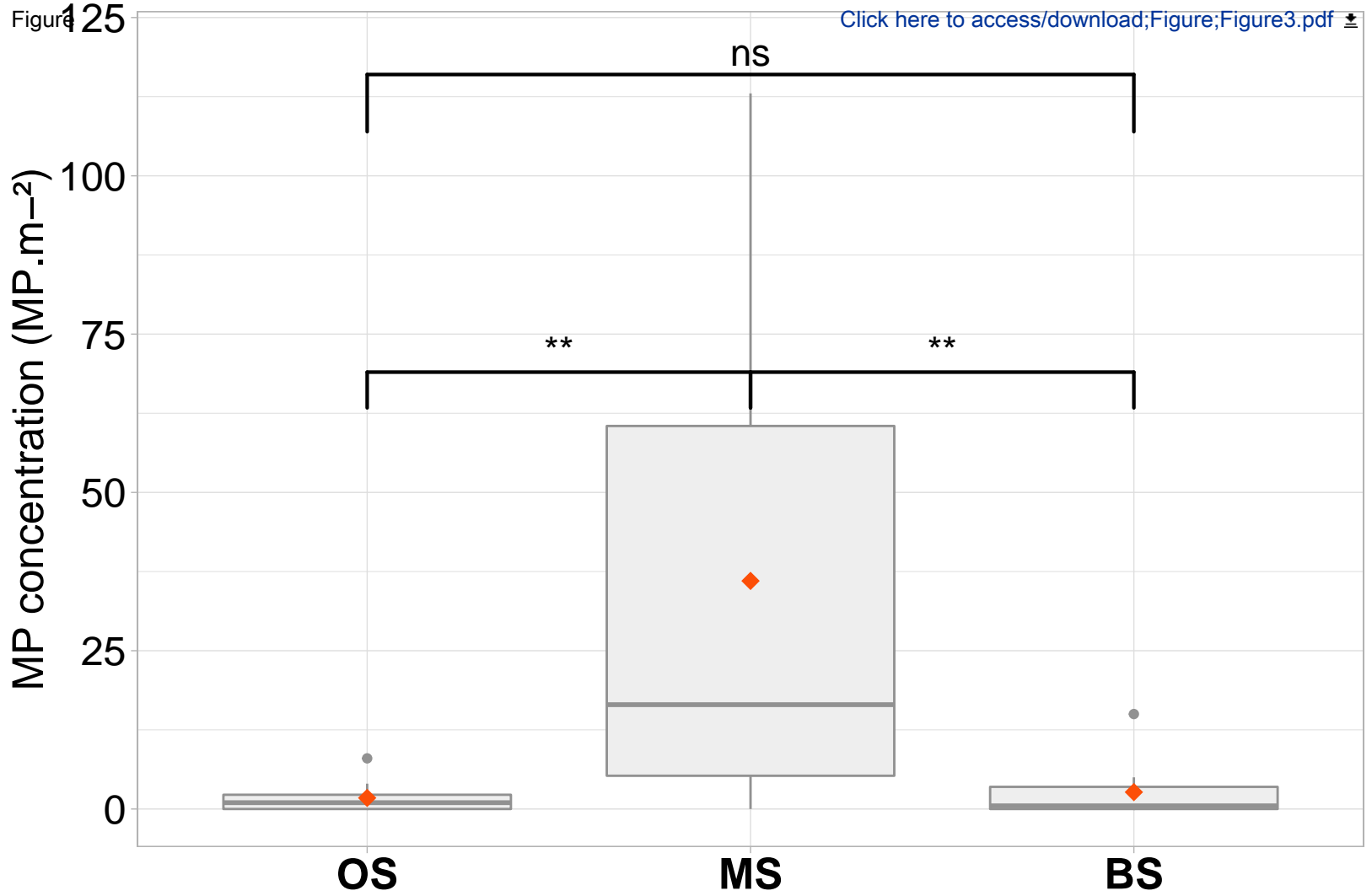
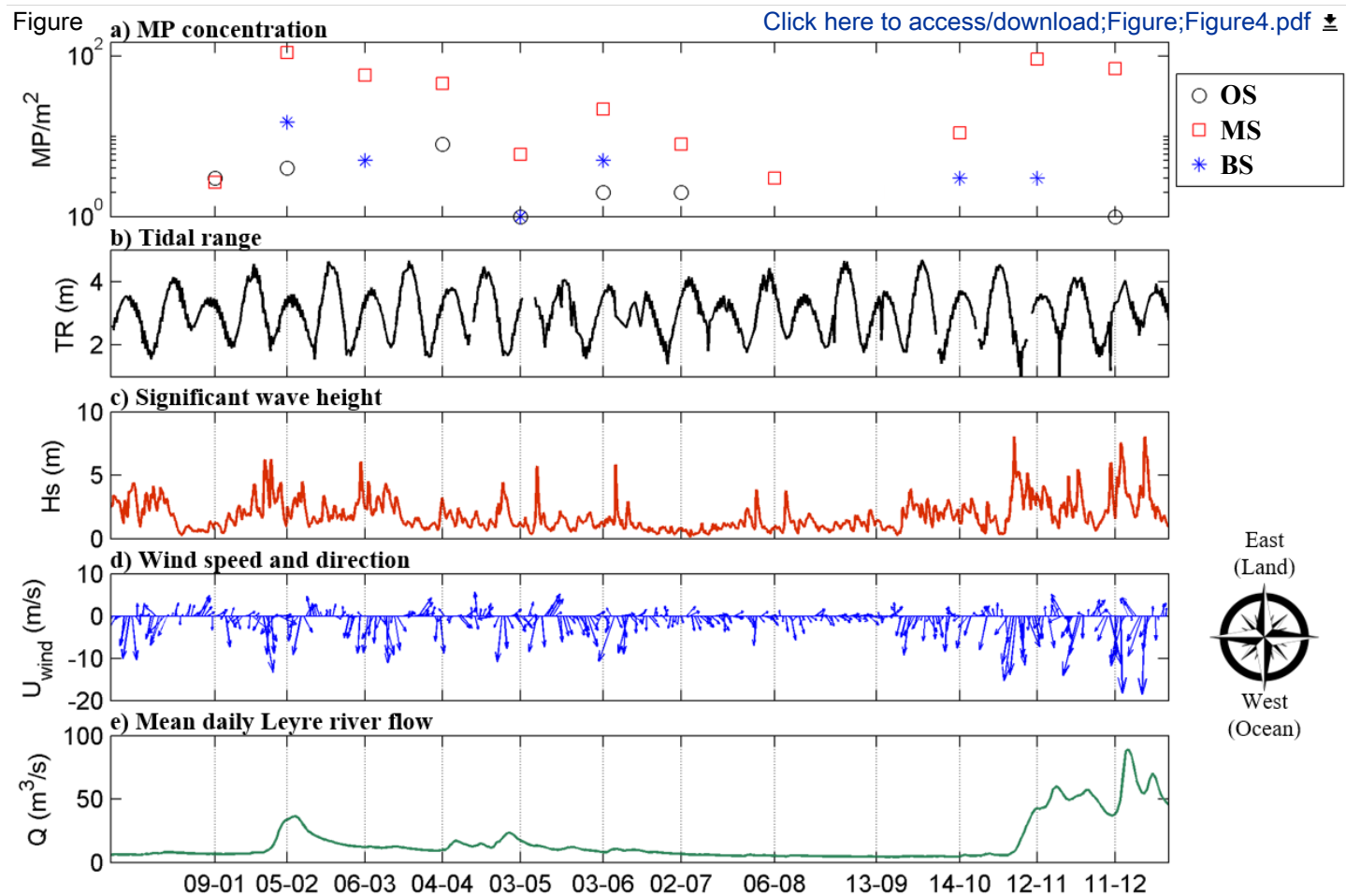


Figure **B)** Polymers PE PP PS EVA PIBMA NP UNK



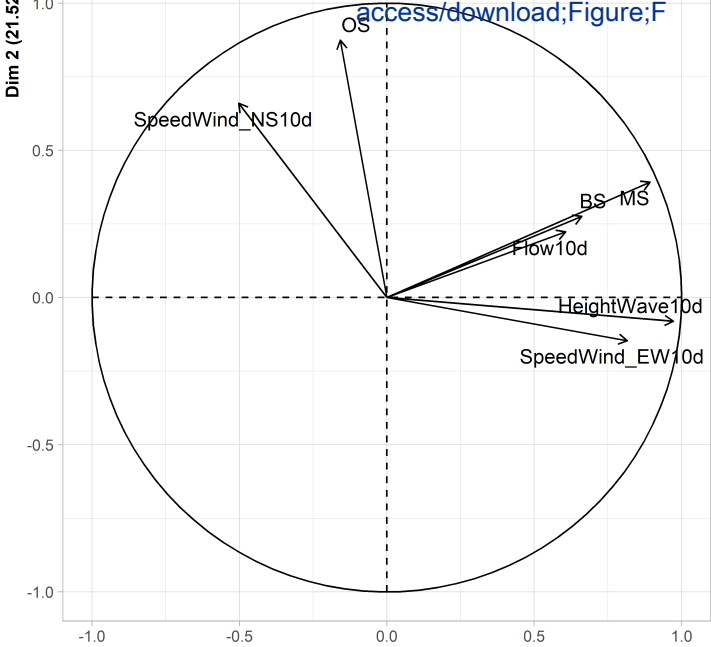






[Click here to access/download;Figure;F](#)

Figure



Dim 1 (49.85%)



Click here to access/download

Supplementary material for on-line publication only
Supplementary Material_STOTEN-D-21-10923 - pour
fusion.docx

This study was conceptualized by BM, JC, SL and CL. Methodologies were set up by BM, JC, SL, IJR and CL. Data validation and duration was made by IJR. MP sampling and statistical analysis and visualization were made by CL. Environmental factors analysis and visualizations were made by IJR and CL. Resources were provided by SV, JC, SL and BM. CL wrote the original draft and IJR, SV, JC, SL, and BM reviewed and edited the manuscript. JC, SL, and BM and SV supervised CL. BM, JC and SL acquired the financial support and BM managed the project. All authors contributed to the article and approved the submitted version.